PERFORMANCE OF NATURAL POZZOLAN-BASED GEOPOLYMER REINFORCED WITH BANANA FIBERS

Kübra Ekiz Bariş,[1] Leyla Tanaçan[2]

ABSTRACT

Türkiye has approximately 50.000 acres of banana plantations. Banana cultivation produces a huge amount of waste that has no commercial value. The main purpose of this study is to investigate the possibilities of using waste banana fiber in natural pozzolan-based geopolymer mortar to increase its ductile fracture behavior. The effects of fiber content and length on physical and mechanical properties were experimentally carried out. The optimum banana fiber content and length were found to be 1.5% and 20 mm, respectively. Above this limit, fibers made it difficult to obtain a workable matrix and generated fiber agglomeration. Although increasing the fiber content from 0.5% to 1.5% and length above 20 mm led to a decrease in the ultrasound pulse velocity, modulus of elasticity and compressive strength due to the higher porosity of the matrix, the increasing ratios of the flexural strength and toughness were consistent. Furthermore, banana fiber-reinforced geopolymer mortars have adequate porosity (22.87%), water absorption ratio (9.25%), swelling thickness (0.58%), saturation coefficient (78%), drying shrinkage ($195x10^{-6}$), water vapor diffusion resistance index (5.73), flexural strength (6.88 MPa), compressive strength (8.75 MPa), and comply with the performance requirements of the related standards. By considering the adequate physical, mechanical and ductile fracture performance of the material, waste banana fiber can be utilized in the production of geopolymers.

KEYWORDS

banana fiber, natural pozzolan, geopolymer, fiber reinforcement.

1. INTRODUCTION

Recent scientific research shows that geopolymer binders can be an alternative to Portland cement [1]. Geopolymer binders are materials that are produced as a result of the reaction of an aluminosilicate source with various alkali activators and have a three-dimensional amorphous structure [2]. The aluminosilicate source and alkali activator are the essential components of

1. Faculty of Architecture and Design, Kocaeli University, Kocaeli, 41310, Türkiye
(Corresponding Author):
E-mail: kubra.ekizbaris@kocaeli.edu.tr
ORCID: https://orcid.org/0000-0002-3830-7185
2. Affiliation: Faculty of Architecture, Istanbul Technical University, Istanbul, 34367, Türkiye.
E-mail: tanacan@itu.edu.tr
ORCID: https://orcid.org/0000-0001-7649-2441

Downloaded from http://meridian.allenpress.com/jgb/article-pdf/19/1/51/3333621/i1943-4618-19-1-51.pdf by greenjournal@verizon.net on 02 March 2024

this binder [1]. Various natural materials, agricultural, industrial, and urban waste materials can be used as sources of aluminosilicate [3]. These binders reduce the environmental impact due to the use of less calcium-based raw materials; they allow for lower production temperatures and less fuel use compared to cement [4]. CO_2 emissions from geopolymer production are approximately 60–80% lower than the emissions released from conventional cement production [5]. However, the production of geopolymers has a higher environmental impact on other impact categories contributing to global warming. This is due to the use of sodium silicate solution as activator. Hence, using materials with a suitable Si/Al molar ratio is under research in geopolymer production [7].

Geopolymer binders have the following advantages, depending on the aluminosilicate source used, alkali activator type, mixing ratio, production, and curing conditions [6, 8, 9]; high compressive strength with a rapid hardening time which may reach 70% of ultimate strength within 4 h, low permeability and shrinkage, long-term resistance to acid and chemical attacks, and thermal stability up to 1200°C [10, 11]. Despite these advantages, one of the most important disadvantages of geopolymers is their brittle behavior, similar to Portland cement. This limits the application areas of geopolymers.

Geopolymers generally include internal micro-cracks, and as a result of these micro-cracks propagating, the tensile strength of geopolymer matrices is likely to be low, potentially leading to brittle failure. Two methods exist for improving the mechanical properties of geopolymer matrices, such as toughness and flexural strength to give ductility and to restrict brittle behavior: one involves adding nanoparticles to the geopolymer mixture, and the other involves using either continuous or short fibers [12]. Studies on steel, inorganic, synthetic, and natural fiber reinforcements of geopolymers are available in the literature. However, more recently, the preference for natural fibers over other fibers in the reinforcing of geopolymers has arisen as a result of the trend toward the production of environmentally benign and energy-saving products [13]. Natural fibers are separated into three main groups: (i) mineral-based; (ii) animal-based; and (iii) plant-based fibers. Since the manufacturing of mineral-based fibers necessitates multiple processing stages before use, like melting and spinning of the minerals at high temperatures, using them in geopolymers may cause significant adverse environmental impact. [14]. Additionally, some fibers made from minerals like asbestos are carcinogenic. On the other hand, because it is challenging to collect animal-based fibers, they are impractical for producing large-scale geopolymers [13]. Plant-based fibers are the most convenient natural fiber type to use in the fabrication of geopolymers because they are more affordable and simpler to use.

Fibers such as glass, carbon, or polyamide are used in high-performance cement composites where high strength and rigidity are required. However, steel, polypropylene, and natural fibers are used in relatively low-cost, energy-saving lightweight cement composites such as blocks, panels, and sheets, especially for social housing or similar construction applications. Although cellulose-based natural fibers are particularly diverse, abundant, and inexpensive, their inherent weaknesses, such as low elastic modulus, high water absorption, susceptibility to fungal and insect attack, and alkali attack from the cement give rise to the relatively poor performance of cement composites. It is therefore necessary to improve the performance characteristics of new natural fiber composites based on geopolymers.

Plant-based fibers are added to brittle matrices in order to enhance the flexural strength by preventing the occurrence and propagation of cracks. Also, they increase the post crack strength, ductility and dimensional stability. A fiber-reinforced material is a two-phase material. The continuous phase is the matrix that holds the fibers together and is defined as the main

Downloaded from http://meridian.allenpress.com/jgb/article-pdf/19/1/51/3333621/i1943-4618-19-1-51.pdf by greenjournal@verizon.net on 02 March 2024

component of the composite due to the excess amount in the composite. The material used as reinforcement in this matrix (i.e., fibers) is the second phase. In materials reinforced with fibers, the mechanical effect on the matrix must be transmitted to the fiber in order for the fiber to participate in load bearing. Here, there is no chemical bond between the fiber and the matrix, and the load transmission takes place by shear force. Therefore, there must be a level of adherence between the fiber and the matrix that can withstand the shear stresses that may occur [15].

Fiber-reinforced composite materials are divided into two types: ductile matrix and brittle fiber or brittle matrix and ductile fiber depending on the properties of the matrix and fiber phases. The fiber ratio is higher in ductile matrix and brittle fiber composites and varies between 20 and 80%. In brittle matrix ductile fiber composites (as in this study), the fiber ratio varies between 0.5 and 5.0%. Fibers of certain lengths can be used in these materials as well as continuous fibers or as layer reinforcement using woven and non-woven layers [13] depending on the requirement. The fiber length therefore varies widely, from a few millimeters to continuous fibers [15].

Longer fibers can improve the strength properties by controlling the spread of macro-cracks, whereas the high proportion of shorter fibers are more densely dispersed in the matrix and can restrict the spread of micro-cracks [12]. The fiber direction is another important factor in terms of the strength of the material and the contribution of fibers to the load transmission. Therefore, oriented fiber-reinforced composites exhibit different properties against loads coming from different directions. In their longitudinal directions, fibers can withstand greater loads [13]. If the fibers are randomly distributed in the matrix, the material is considered isotropic, and the properties do not change depending on the direction [15].

There have been more studies published recently that investigate the use of plant-based fibers to improve the mechanical properties of geopolymer materials. Researchers have studied various plant-based fibers such as sisal [16, 17], coir [17], jute [16], musa basjoo [19], cotton [20, 21], hemp [22], and sugarcane bagasse [23, 24]. However, the number of studies regarding the incorporation of banana fibers in geopolymer mortars is still limited [12].

This experimental study aims to fill the current knowledge gap by incorporating banana fibers in natural pozzolan-based geopolymer mortars. In the scope of the study, a comprehensive evaluation of the effects of various contents and lengths of banana fiber on the physical and mechanical properties of natural pozzolan-based geopolymers was carried out. There are approximately 50.000 acres of banana plantations in the Anamur and Bozyazı regions of Türkiye, and 400.000 tonnes of bananas are cultivated per year. Banana cultivation produces a huge amount of waste. Only in Anamur and Bozyazı in Türkiye are approximately 18.000 tonnes of banana waste generated in one crop season. This waste fiber has no commercial significance, and there is a serious issue with the CO_2 emissions during transportation to landfills. Furthermore, each tonne of this waste fiber, left to decompose, emits about half-tonne of CO_2 annually [25]. Thus, the incorporation of banana fibers in geopolymers might provide a useful and efficient method of managing this agricultural waste which would otherwise be harmful to the environment. Besides, biomaterials derived from plants including wood and agricultural by-products sequester carbon over the course of their lifetime and this carbon remains stored in the materials until the materials biodegrade or combustion. Local sourcing is important, otherwise carbon emissions from transportation can significantly drive up the embodied emissions. Hence, the evaluation of this low-cost, biodegradable, renewable, nontoxic, and easy-to-process fiber in building material production would have a sustainable benefit in terms of substantial local availability [24].

Downloaded from http://meridian.allenpress.com/jgb/article-pdf/19/1/51/3333621/i1943-4618-19-1-51.pdf by greenjournal@verizon.net on 02 March 2024

2. MATERIALS AND METHODS

2.1 Materials

To develop the geopolymer mortar, natural pozzolan was used as an aluminosilicate source and was mined from the Datça Peninsula in Türkiye. It was then dried at 55°C for 24 h before being pulverized into particles that were 95% smaller than 90 μm. It had a specific gravity of 2.52 g/cm^3 and a remarkably high specific surface area (5467 cm^2/g). Table 1 displays the chemical characterizations that were attained using X-ray fluorescence spectrometer (XRF). Pozzolanic oxides (SiO_2 and Al_2O_3) are the most prevalent oxides, followed by K_2O and Na_2O. The qualitative phase (mineralogical) characteristics of the natural Datça Pozzolan was studied by means of X-ray diffraction (XRD) analysis conducted using D8-Advance Bruker-XRD equipment with Cu X-ray tube (1.5406 Angstrom). According to the XRD data, anorthite, quartz, feldspar and microcline are observed (Figure 1).

Liquid sodium silicate (Na_2SiO_3 = SiO_2/Na_2O = 3.2) and 12.5 molar (M) potassium hydroxide (KOH) were used for alkaline activation. KOH solution was made by dissolving KOH pellets in distilled water and allowing them to cool for 24 h before adding them to the mixture. Standard quartz sand with the largest grain size of approximately 2.0 mm was used to produce geopolymer mortar.

The banana fiber used in this research is a waste product of banana cultivation and was obtained from Bozyazı, Anamur region in Türkiye. Banana fibers consist of 31.5% cellulose, 15% hemicellulose, 15% lignin, and 38.5% other substances by weight [26]. They have a density of about 1.35 g/cm^3, a tensile strength of 355 MPa, an elastic modulus of 33.8 GPa, and an elongation at failure of about 5.30% [26]. Longitudinal slices were manually scraped from the banana stalks (Figure 2a), and these slices were fed to a fiber extracting machine. When the fiber extracting machine ran, the fiber juice was extracted and the fibers were obtained (Figure

TABLE 1. Chemical analysis of the natural Datça Pozzolan (wt.%).

Datça Pozzolan	SiO_2	Al_2O_3	Fe_2O_3	CaO	MgO	P_2O_5	K_2O	Na_2O	TiO_2	MnO_2	Cr_2O_3	NiO
	75.29	15.99	0.98	1.22	0.62	0.07	3.02	2.21	0.14	0.04	0.005	0.004
	CuO	ZnO	Rb	SrO	Y_2O_3	ZrO_2	Nb_2O_5	BaO	Cl	SO_3	LOI	Total
	0.002	0.002	0.006	0.015	0.002	0.01	0.001	0.097	0.092	0.1	0.15	100

FIGURE 1. X-ray diffraction (XRD) analysis of the natural Datça Pozzolan.

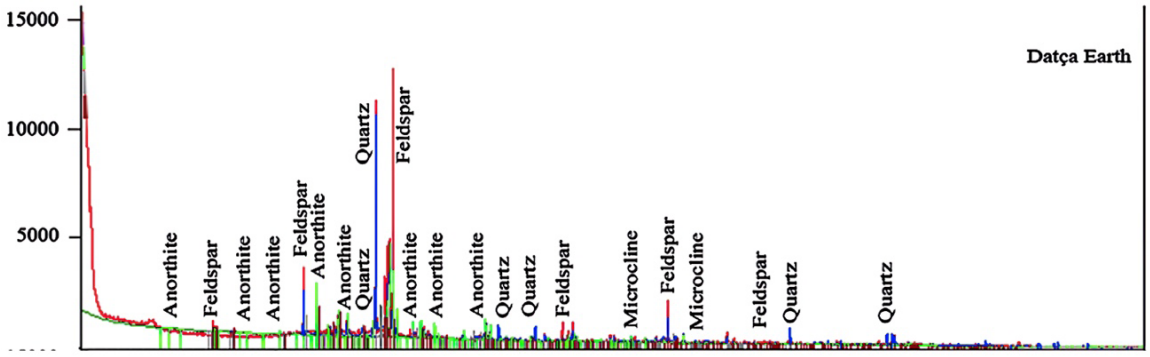

Downloaded from http://meridian.allenpress.com/jgb/article-pdf/19/1/51/3333621/i1943-4618-19-1-51.pdf by greenjournal@verizon.net on 02 March 2024

2b). Afterwards, they were dried at 50°C for 24 h and cut into lengths of 10, 15, 20, and 25 mm, respectively (Figure 2c).

2.2 Mixing Ratio

Unreinforced geopolymer mortars and fiber-reinforced geopolymer mortars were produced to investigate the effect of fibers on physical and mechanical properties. In a previous study conducted by the authors of this research, the ideal mixing ratios that allowed the production of Datça pozzolan-based (Earth of Datça-ED) geopolymer binder with the highest physical and mechanical properties were taken as the basis. Accordingly, sodium silicate (SS)-to-KOH (activator ratio), total alkali activator-to-binder, and dry pozzolan-to-standard sand ratios by weight are 2.5, 0.30, and 0.33, respectively.

The geopolymer mortars were reinforced with banana fibers, with the contents varying between 0% and 0.5, 1.0, and 1.5% by weight of the natural pozzolan (ED). Unreinforced mortar (0% fiber content) was used as the control mixture. The maximum fiber content was constrained by the mortar's workability to avoid adverse casting conditions brought on by challenges with molding, vibrating, and compacting [16]. The maximum amount of water to produce a workable consistency of the fresh control mortar was identified with the flow table test in conformity with TS EN 12350-5 [27]. To determine the flow value, a hollow cone having

FIGURE 2. Longitudinal slices that were scraped from the banana stalks (a); extraction of fibers from the machine (b); and 25 mm banana fibers after drying (c).



Downloaded from http://meridian.allenpress.com/jgb/article-pdf/19/1/51/3333621/i1943-4618-19-1-51.pdf by greenjournal@verizon.net on 02 March 2024

a base diameter of 200 mm, top diameter of 130 mm, and height of 200 mm was placed on the flow table. The fresh mixture was filled into the cone by tamping slightly ten times with the tamping bar. After waiting 20 s, the cone was raised vertically by the handles. Afterwards, the rotating handle of the table was revolved until 15 drops, each drop taking 1 s. Finally, the maximum dimension of the mortar spread in the two directions (d1, and d2, in mm) was recorded and the flow value was calculated using Eq. 1:

$$f = [(d1 + d2)/2] \quad \text{(Eq.1)}$$

Accordingly, the flow was found to be 120. The addition of fiber lowers the workability of the mixture, however, the water-to-binder ratio was kept constant in all fiber reinforced mortars because adding more water to compensate for the workability loss caused by the existence of fibers may worsen the mechanical properties [16].

2.3 Mixing, Curing, and Testing Methods

Natural pozzolan (ED), standard sand, and banana fibers (Figure 3a) were dry-mixed with a mixing machine at low speed for 10 minutes to provide a uniform distribution of fibers in the matrix (Figure 3b). As the mixing continued, the alkali activators were added gradually and mixed for an additional 3 minutes until a homogenous mortar was obtained (Figure 3c). The fresh mortar was cast into prismatic molds with dimensions of 40×40×160 mm and covered with polyethylene (PE) to avoid rapid loss of moisture. The mortars were cured at 70°C and 95±5% RH for 24 h. After 24 h, the specimens were demoulded and left to air curing at 20°C and 55±5% RH until the day of testing at 28 days.

The specimens were coded using the [X-X] system: the first "X" shows the content of the banana fiber by weight, and the second "X" indicates the fiber length, in mm. Three specimens were produced for each test, whereas the compressive strength test was performed on six specimens. The specimens were tested for unit weight (Δ) in accordance with TS EN 1015-10 [28], water absorption under atmospheric pressure (S_a) in accordance with TS EN 13755 [29],

FIGURE 3. Incorporation of banana fibers in natural pozzolan and sand (a); dry-mixing with a mixing machine of the components until a homogenous mortar was obtained (b); the fresh mortar after alkali activator addition (c).



Downloaded from http://meridian.allenpress.com/jgb/article-pdf/19/1/51/3333621/i1943-4618-19-1-51.pdf by greenjournal@verizon.net on 02 March 2024

and swelling in water in accordance with ISO 8335 [30]. The porosity of the specimen was determined according to the following formula (Eq. 2):

$$P = [1 - (\Delta/p) \times 100 \quad \text{(Eq. 2)}$$

where (Δ) is the unit weight and ρ is the specific weight of the specimen, (g/cm^3). The specific weight is the mass of the unit volume of the dried material in the void-free state and was determined according to TS 699 [48].

Drying shrinkage was tested until 90 days of curing period in accordance with TS EN 1920-8 [32]. Following demoulding, the length change of each specimen was measured on each of the following air curing days: 1, 2, 3, 4, 5, 6, 7, 15, 22, 30, 40, 50, 60, 70, 80, and 90 days. The water vapor diffusion resistance index (WVDRI) (μ) was tested in accordance with TS EN 12086 [33].

The dynamic ultrasound pulse velocity (UPV) test was performed using a portable ultrasonic non-destructive equipment (Proceq) in compliance with TS EN 14579 [31]. Non-destructive ultrasound testing is based on the introduction of longitudinal ultrasonic waves (from $2\times10^4\pm10^3$ Hz) by periodic pulses using a transducer (emitter) coupled to the surface. After traveling through the material, the waves are collected by another transducer (receiver). When the pulse is coupled into the material, it undergoes multiple reflections at the boundaries of the different material phases within the material. A complex system of stress waves is developed, which includes both longitudinal and shear waves propagating through the material. The velocity of ultrasonic pulses is influenced by the ambient temperature (<5°C and >30°C), mineralogical composition, heterogeneity, discontinuity, intercrystalline connections and density of the material. The presence of hollows, fissures, or cracks within the material is reflected by a drop in the velocity as a result of absorption and dispersion. The pulse velocity (V) (km/s) was calculated by (Eq. 3):

$$V = l/t \quad \text{(Eq. 3)}$$

where (l) is the length of the specimen in m (distance between emission and reception) and (t) is the time in μs elapsed by the pulse to transverse the length to reach the receptor. The pulse velocity (V) of longitudinal stress waves in a material is related to its elastic properties and density according to the following formula (Eq. 4):

$$MoE = (10^5 \times V^2 \times \Delta)/g \quad \text{(Eq. 4)}$$

where (MoE) is the dynamic modulus of elasticity (GPa), (Δ) is the unit weight of the material (kg/dm^3) and (g) is the gravitational acceleration (9.81 m/s).

The flexural (R_f) and compressive (R_c) strength tests were performed in accordance with TS EN 196-1 [34]. In addition, the effects of fiber incorporation on the toughness and fracture behavior of the specimens were determined with flexural load-displacement curves. Table 2 presents the test results.

Downloaded from http://meridian.allenpress.com/jgb/article-pdf/19/1/51/3333621/i1943-4618-19-1-51.pdf by greenjournal@verizon.net on 02 March 2024

TABLE 2. The test results of the specimens.

Specimen code	Flow	Unit weight (Δ) (g/cm^3)	Porosity (P) (%)	Water absorption (S_a) (%)	Open porosity (S_h) (%) (S_a*Δ)	Swelling thickness (%)	Saturation coefficient (SC) (%) (S_h/P)	Ultrasound pulse velocity (UPV) (km/s)	Modulus of elasticity (MoE) (GPa)	Water Vapor diffusion resistance index (WVDRI) (μ)	Compressive strength (R_c) (MPa)	Flexural strength (R_f) (MPa)
00–00 (Ref)	120	2.01	20.55	8.83	17.74	0.28	79	2.16	9.55	7.74	9.25	1.81
0.5–10	93	1.95	22.62	9.23	17.99	0.34	79	2.10	8.76	7.16	9.02	4.28
0.5–15	90	1.96	22.53	9.10	17.83	0.33	79	2.12	8.97	7.25	9.15	5.17
0.5–20	87	1.97	22.31	9.01	17.74	0.34	79	2.13	9.11	7.38	9.20	5.82
0.5–25	84	1.92	23.57	9.97	19.14	0.35	81	2.08	8.46	6.51	7.42	4.75
1.0–10	70	1.93	23.21	9.34	18.02	0.42	77	2.08	8.51	6.58	8.64	4.56
1.0–15	66	1.94	22.86	9.23	17.90	0.41	78	2.11	8.80	6.82	8.86	5.44
1.0–20	62	1.95	22.54	9.14	17.82	0.43	79	2.12	8.93	6.90	8.99	6.38
1.0–25	58	1.90	24.11	10.17	19.32	0.43	80	2.05	8.13	6.40	7.00	5.12
1.5–10	58	1.92	23.45	9.41	18.06	0.57	77	2.06	8.30	5.57	8.31	4.82
1.5–15	54	1.93	23.07	9.33	18.00	0.57	78	2.10	8.67	5.62	8.58	5.74
1.5–20	50	1.94	22.87	9.25	17.94	0.58	78	2.11	8.80	5.73	8.75	6.88
1.5–25	45	1.88	24.89	10.36	19.47	0.58	78	2.03	7.89	5.53	6.43	5.49

Downloaded from http://meridian.allenpress.com/jgb/article-pdf/19/1/51/3336211/1943-4618-19-1-51.pdf by greenjournal@verizon.net on 02 March 2024

3. RESULTS AND DISCUSSION

3.1 Effects of Fiber Content and Fiber Length on the Development of Physical Properties of Banana-Fiber Reinforced Geopolymers

3.1.1 Workability

The flow of the mortars with 0.5, 1.0, and 1.5% fiber content as functions of fiber length is given in Figure 4.

The inclusion of banana fibers significantly decreased the workability of mortars with the same w/b ratio. Even the inclusion of 0.5% fiber in the matrix reduced the flow to the 93–84% range, changing according to the increase in fiber length from 10 to 25 mm compared to the control specimen (00–00), which has a flow of 120. The flow reduced as the fiber length and fiber content increased. The flow reduction rate between 0.5 and 1% fiber content is approximately 50% higher than the flow reduction rate between 1 and 1.5% fiber content.

The addition of more fibers made the fresh matrix stiffer. This may be due to the porous structure and considerable moisture absorption of the hydrophilic banana fibers [12] and the large shear force between the geopolymer matrix and fiber, which further reduced fluidity and workability [35]. The flow test therefore identified the maximum content of banana fiber that could be added to the natural pozzolan-based geopolymer matrix as 1.5%. Because it was not possible to add more banana fiber to the matrix, which otherwise would make the fresh mortar difficult to mix, cast, and mold. This finding is consistent with the findings of: (i) Wongsa et al. [17] who determined that the addition of sisal and coconut fibers (up to 1.0 vol%) decreased the workability of fly ash-based geopolymer mortars; (ii) Alomayri et al. [20, 21] who explained that geopolymer pastes reinforced with cotton fibers (up to 1.0 wt%) exhibited low workability; and (iii) Su et al. [18] who reported that the increase in the content of lignin fiber (up to 1.25 wt%) led to the decrease of the workability of fly ash/slag-based geopolymers; and (iv) Reddy et al. [19] who determined that incorporation of musa basjoo fibers (up to 1.5 wt%) caused the loss of workability of the ash-based geopolymer concrete.

The 0.5 increment of the fiber length drops the flow; a higher reduction of flow was obtained with the higher fiber content (1.5%-0.77 times), than the 0.5% (0.93 times). Longer

FIGURE 4. The flow of the mortars with 0.5, 1.0, and 1.5% fiber content as functions of fiber length.

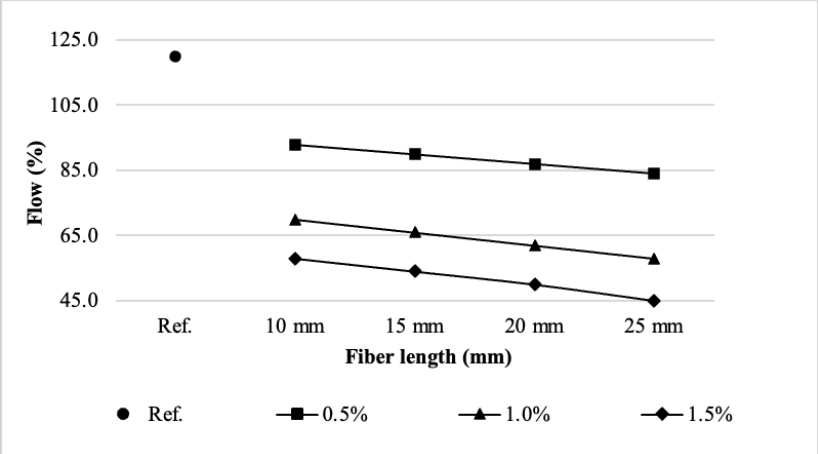

Downloaded from http://meridian.allenpress.com/jgb/article-pdf/19/1/51/3333621/i1943-4618-19-1-51.pdf by greenjournal@verizon.net on 02 March 2024

fibers together with higher fiber content not only made it difficult to obtain a homogeneous matrix during the mixing of the mortar but also caused lower fiber dispersion in the matrix compared to the shorter fibers.

3.1.2 Porosity and Unit Weight

Porosity is a crucial property that significantly affects other mechanical and physical characteristics of a material. The porosity (P) and unit weights (Δ) of the mortars with 0.5, 1.0, and 1.5% fiber content as functions of fiber length are given in Figure 5.

Fiber inclusion in the matrix at 0.5, 1.0, and 1.5% gradually increased the P while decreasing the (Δ) of the mortars. The highest fiber content had the highest Ps and the lowest (Δ)s. The porosity, which was found to be 20.55% for the reference specimen, increased to a range of 22.31–24.89% with the increase in fiber content and fiber length. (Δ) of the reference specimen was found to be 2.01 g/cm^3. Parallel to the behavior of P, the (Δ)s of the fibrous mortars decreased to the range of 1.97–1.88 g/cm^3. The specimen with the highest banana fiber incorporation (1.5%) and fiber length (25 mm) had the highest P (24.89%) and the lowest (Δ) of 1.88 g/cm^3. One reason for this increase in porosity is that natural banana fiber has a porous structure. Another reason is the presence of entrapped air that resulted from the addition of fiber to the fresh matrix. The existence of this entrapped air would increase the number of voids in the matrix [24]. Moreover, in specimens having higher fiber concentrations (i.e., 1.5%), the fibers have a tendency to cluster together throughout mixing, entrapping water-filled areas which eventually turn into pores [21]. The tendency to increase in porosity with increasing fiber content is consistent with the results of other studies with coir [17], sisal [17], cotton [20], and sugarcane bagasse [24] plant-based fibers.

On the other hand, one of the reasons for the decrease in (Δ) was that the matrix with the highest density in the unreinforced state was replaced by the lower density (1.35 g/cm^3) banana fiber. In addition, entrapped air that was produced during the mixing of the fibers in the matrix probably contributed to this reduction [22]. Furthermore, when the fiber content was increased, the fibers clumped together during mixing creating interstitial pores within the

FIGURE 5. (P)s and (Δ)s of the mortars with 0.5, 1.0, and 1.5% fiber content as functions of fiber length.

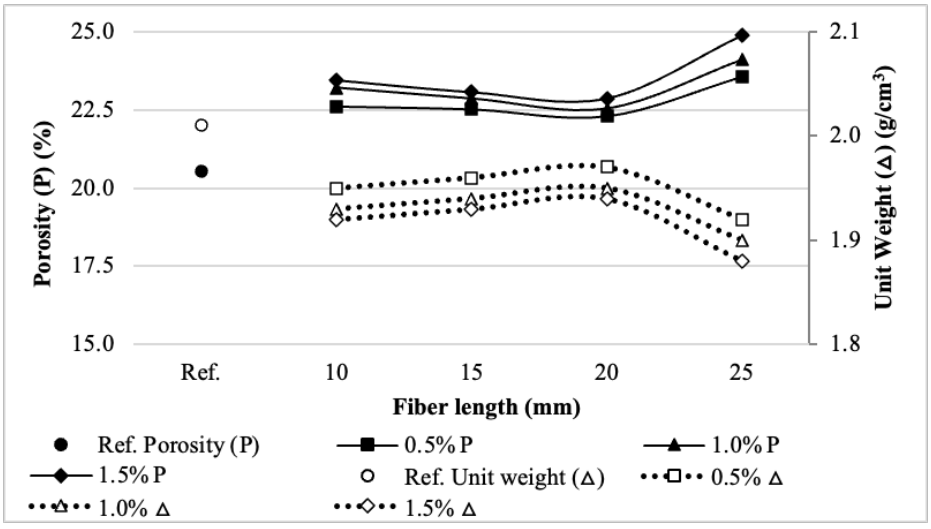

Downloaded from http://meridian.allenpress.com/jgb/article-pdf/19/1/51/3333621/i1943-4618-19-1-51.pdf by greenjournal@verizon.net on 02 March 2024

matrix. When the matrix is in a fresh state, the pores usually fill with water. However, when the matrix dries, the water evaporates making the mortar porous and less dense, which also has an adverse impact on its mechanical properties [35]. The decreasing density with increasing fiber contents is also in agreement with other studies regarding coir-based [17], sisal-based [16, 17], jute-based [16], cotton-based [20], hemp-based [22], and sugarcane bagasse-based [24] fiber-reinforced geopolymer composites.

A slightly higher reduction rate of the (Δ)s between 0.5 and 1.0% fiber content was observed than the reduction rate between 1.0 and 1.5% fiber content, as happened in the flow properties. Doubling the initial 0.5% fiber content to 1.0% was more effective on flow and (Δ) than the second addition of the same amount of fiber. Above the 1.0% fiber content, there was no significant reduction of (Δ) observed.

Up to a fiber length of 20 mm, there is a gradual decrease in P values and an increase in (Δ)s. What is interesting is that there is a sharp drop in both properties observed at 20 mm fiber length, which may be accepted as the critical fiber length. This may reveal that the interaction between banana fibers and matrix reached its maximum degree at the critical fiber length and the influence of length decreased with longer fibers, possibly due to fiber entanglement [36]. Hence, in all fiber contents (0.5, 1.0, and 1.5%), the highest P and lowest (Δ) values were obtained at 25 mm fiber length. Banana fibers with a 25-mm length made it difficult to obtain a homogeneous matrix during the mixing of the mortar and caused lower dispersion and fiber agglomeration in the matrix, which can be seen in Figure 9c in the digital images of the specimens.

3.1.3 Water Absorption Ratio under Atmospheric Pressure

Water absorption (S_a) of the mortars with 0.5, 1.0, and 1.5% fiber content as functions of fiber length is given in Figure 6.

The lowest value of the (S_a) (8.83%) was found in the unreinforced reference geopolymer mortar. The highest water intake increased as the fiber content increased. The reinforcement

FIGURE 6. (S_a) of the mortars with 0.5, 1.0, and 1.5% fiber content as functions of fiber length.

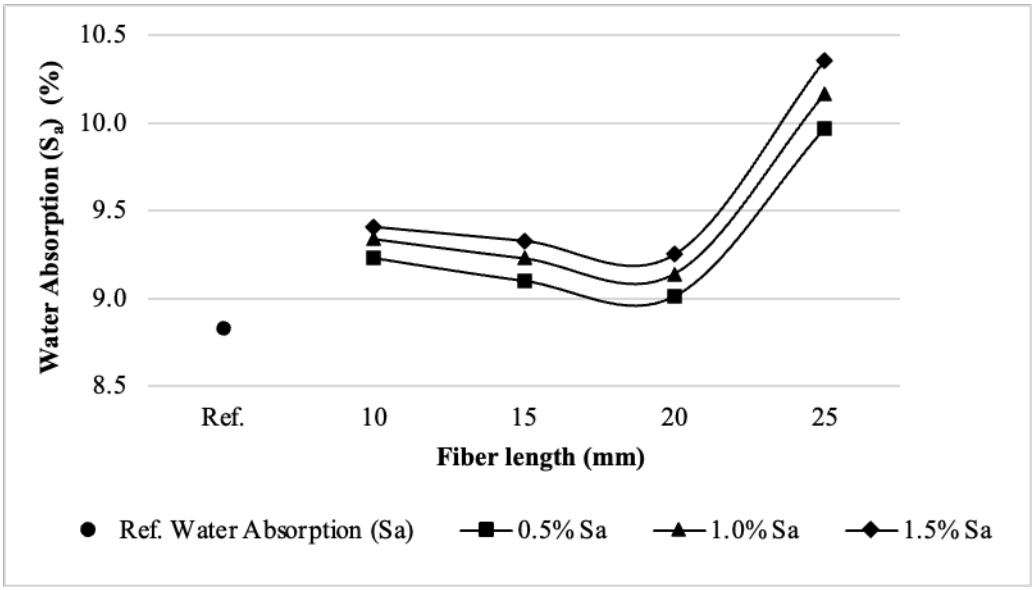

Downloaded from http://meridian.allenpress.com/jgb/article-pdf/19/1/51/3333621/i1943-4618-19-1-51.pdf by greenjournal@verizon.net on 02 March 2024

of mortars with banana fiber at contents ranging from 0.5% to 1.5% resulted in an increase in the (S_a) in the range of 9.01–10.36%. The specimen containing the highest content of banana fiber (1.5%) and the highest length (25 mm) had the highest (S_a) of 10.36%, which may be due to the increased porosity of the matrix and the higher water absorption capacity of the hydrophilic fibers themselves [22].

Microcracks allow water molecules to penetrate the mortar in a moist environment, and the fiber's hydrophilic characteristics enable the fiber to absorb this water [37]. When water molecules attach to plant fibers' hydrophilic groups, a considerable amount of hydrogen bonds are produced, creating a physical barrier between the fiber and the matrix and lowering the adhesion at the interface [38]. As a result, the fibers swell, which may result in microcracks in the matrix and fiber debonding from the matrix [37]. Other geopolymer mortars with coir [17], sisal [16, 17], hemp [22], and sugarcane bagasse [24] fibers also showed an increasing trend in the (S_a) because of the increased fiber content.

Increasing the fiber length from 10 mm to 15 and 20 mm caused a slight decrease in the (S_a), parallel to the results obtained in terms of a gradual decrease in porosity and an increase in the unit weight of the material. However, further increasing the fiber length to 25 mm significantly increased the (S_a). This result was due to the fact that the agglomeration of 25-mm banana fibers in the matrix during the mixing process created interstitial pores inside the matrix.

Given that the porosity (P) is higher than the water absorption ratio (Sa), it is understood that although water penetrates the sample immersed in water, it could not fill all the gaps. The micro and gel pores, which are smaller than 0.1 μm, are too small so that water could not penetrate into them. On the other hand, when the pores are not interconnected, water could not reach the pores in the middle part of the sample. Apart from these, the water advancing in the pores may not continue its progress in the face of the resistance of compressed air here. These explanations demonstrate that (S_a) really represents a value less than the total void ratio in the material. In fact, for instance, the (S_a) of the specimen (0.5–10), whose P was 22.62%, was determined as 9.23%. When 17.99% of the same specimen water absorption ratio by volume (S_h) is taken into account, it can be inferred that some of the material's pores were filled by water and the rest filled by air.

Dimensional changes such as a high level of swelling can negatively affect the material's mechanical properties owing to the development of internal microcracks [39]. Therefore, in accordance with ISO 8335 [30], the swelling thickness percentage of the materials that were submerged in a water-filled tank for 24 h shall be less than 2%. As demonstrated in Table 2, the lowest thickness of swelling (0.28%) is obtained with the unreinforced specimens, and the gradual inclusion of banana fiber resulted in an increase in swelling thicknesses ranging from 0.33 to 0.58%, which still comply with the standard requirement.

The ratio of the water absorbed by the material at atmospheric pressure to the material's total porosity is indicated by the saturation coefficient (SC), a crucial property of the material's resistance to frost. If the capillary cavities of the material are entirely filled with water, and when water freezes, it cannot find a space to increase its volume by 10%, which might cause surface delamination, disintegration, or cracking of the material. The material sustains its stability under the effect of freezing if the pores are 80% water-saturated at most because there is adequate space for the water to expand when it freezes. As a consequence, whether the saturation coefficient is 80% or less determines the material's ability to withstand frost. In all specimens, (SC)s were found equal to or lower than 80%, indicating that mortars are frost-resistant, as shown in Table 2.

Downloaded from http://meridian.allenpress.com/jgb/article-pdf/19/1/51/3333621/i1943-4618-19-1-51.pdf by greenjournal@verizon.net on 02 March 2024

3.1.4 Ultrasound Pulse Velocity and Young's Modulus of Elasticity

Ultrasound pulse velocity (UPV) and Young's modulus of elasticity (MoE) values of the mortars with 0.5, 1.0, and 1.5% fiber content as functions of fiber length are given in Figure 7.

A nondestructive test method used to assess a material's homogeneity is the (UPV) [40]. Material with pores and cracks has a lower UPV, which aids in determining its quality [41]. As the compressive strength increased, the UPV of fly ash-based geopolymer concrete tended to increase, according to earlier studies that investigated the UPV to determine concrete quality [17]. The findings on compressive strength from the current research were also compatible with the UPV values (Figure 12).

The highest UPV (2.16 km/s) was determined in the unreinforced reference geopolymer mortar, as expected. It should be highlighted that the results were affected by the presence of banana fibers because ultrasonic waves propagated through the fibers more slowly than they did through the matrix. The reinforcement of the mortar with banana fiber at contents ranging from 0.5% to 1.5% resulted in a decrease in the UPV in the range of 2.03–2.12 km/s. This was owing to the higher porosity and a lower density of banana fiber-reinforced geopolymers than those of the unreinforced matrix. In other words, the material contained voids that would absorb or disperse sound, slowing it down, and the structure shifted away from being homogeneous.

The highest MoE (9.55 GPa) was determined in the unreinforced geopolymer mortar. With the incorporation of banana fibers and the gradual increase in fiber content and length, the (MoE) of the mortar decreased in parallel with (UPV). Increasing fiber length from 10 mm to 15 and 20 mm showed a slight increase in UPV and MoE values parallel to the gradual decrease in porosity and increase in density. This could indicate that the interaction between banana fibers and geopolymer matrix achieves its peak level at 20-mm fiber length. However, further increasing fiber length to 25 mm led to a sharp reduction in UPV and MoE. In all fiber contents (0.5, 1.0, and 1.5%), the lowest UPV and MoE values were obtained at 25 mm fiber length. The main reason for this was that, as determined by other physical properties,

FIGURE 7. (UPV) and (MoE) of the mortars with 0.5, 1.0, and 1.5% fiber content as functions of fiber length.

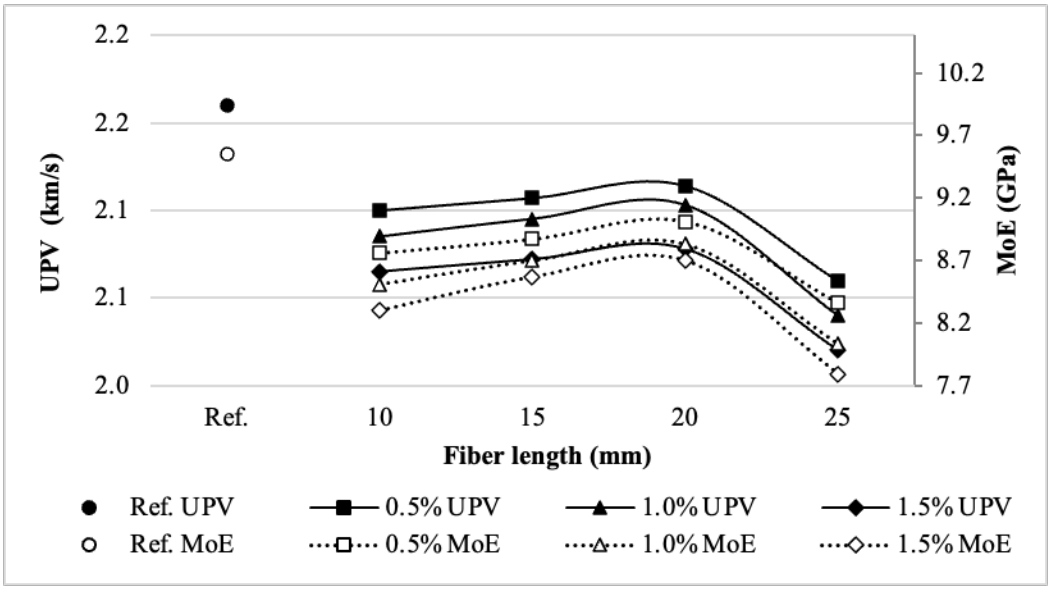

Downloaded from http://meridian.allenpress.com/jgb/article-pdf/19/1/51/3333621/i1943-4618-19-1-51.pdf by greenjournal@verizon.net on 02 March 2024

the 25-mm banana fiber prevented obtaining a homogeneous matrix during the mixing of the mortar, and the agglomeration of the fibers created more voids in the matrix.

Compressive strength, flexural strength, UPV, and MoE of the material enhanced parallel with the increase in the fiber length from 10 to 15 and 20 mm, but decreased with the increase in the fiber content from 0.5 to 1 and 1.5%. While this trend was conserved, a sharp drop was observed in the mechanical properties of the material above 20 mm (25 mm) fiber length, which was also tracked by the decrease in UPV as well as MoE. The inclusion of a fiber of 25 mm into the matrix reduced the workability of the fresh mortar and probably created interstitial pores within the hardened material, which reduced the ultrasonic pulse velocity travelling through the material and its mechanical properties. As such, there is also a good correlation between the pulse velocity and mechanical strengths as a measure of material quality.

By measuring the (UPV) in two separate areas of the same specimen, it was possible to determine the homogeneity of the fiber dispersion inside the geopolymer matrix. Following that, the homogeneity percentage was determined using the standard deviation of the (UPV) results. As expected, the unreinforced mortar had the highest homogeneity (99.5%); the incorporation of banana fibers and the increase in fiber content led to a decrease in the homogeneity of the geopolymer mortar (Figure 8a).

When the fiber content was kept constant at 0.5%, the increase in fiber length from 10 to 25 mm caused a gradual decrease in homogeneity ratio as shown in Figure 8b. The lowest homogeneity (82.4%) was determined in the specimens with the longest fiber length (25 mm). In specimens with 25 mm fiber length, lower dispersion and fiber agglomeration (balling of fibers) were also observed with digital images of the specimens (Figure 9c).

Digital images of the reference, 0.5–20, and 0.5–25 specimens were observed by optical microscopy (10x) and are given in Figure 9. These images were also found in conformity with homogeneity percentages. The reference specimen has the most homogeneous appearance

FIGURE 8. UPV and homogeneity of the mortars as functions of fiber content and fiber length: (a) effect of fiber content at 20 mm fiber length; (b) effect of fiber length at 0.5% fiber content.

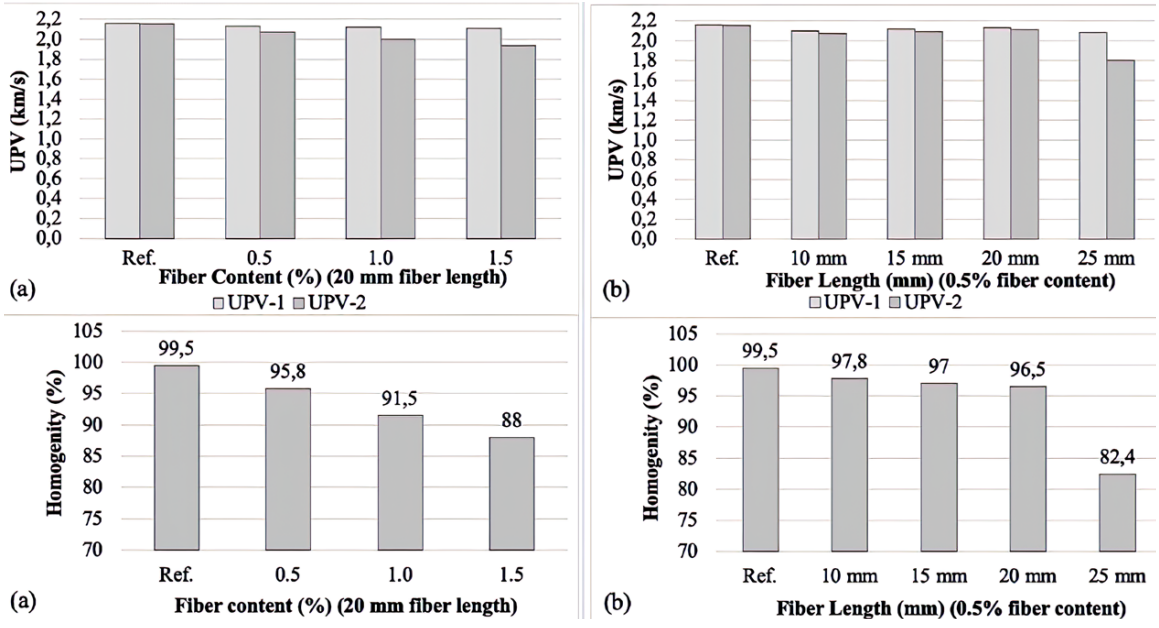

Downloaded from http://meridian.allenpress.com/jgb/article-pdf/19/1/51/3333621/i1943-4618-19-1-51.pdf by greenjournal@verizon.net on 02 March 2024

(Figure 9a), whereas the mortar coded as (0.5–20) has a lower but more consistent appearance with its 96.5% homogeneity (Figure 9b). Banana fiber with 25-mm length made it difficult to obtain a homogeneous matrix during the mixing of the mortar, which caused lower dispersion and fiber agglomeration in the matrix (Figure 9c).

3.1.5 Water Vapor Permeability

Diffusion is the process by which water vapor migrates through a material. In practice, a maximum allowable rate of 15 is the accepted water vapor permeable standard [47]. The water vapor diffusion resistance index (WVDRI) (μ) was measured to determine the water vapor permeability of the mortars. The water vapor diffusion resistance index (WVDRI) (μ) of the mortars with 0.5, 1.0, and 1.5% fiber content as functions of fiber length are given in Figure 10.

It can be seen in Figure 10 and Table 2 that the vapor diffusion resistance coefficients of banana fiber-reinforced geopolymers range from 5.53 to 7.74. The highest value of (μ) is found in the unreinforced geopolymer mortar (7.74), which contains no banana fibers. The introduction of banana fiber at contents ranging from 0.5% to 1.5% resulted in a decrease in (μ) in the range of 5.53–7.38 when compared to the unreinforced specimen. In addition, increasing fiber content decreased the (μ) value. The specimen with the highest banana fiber incorporation (1.5% fiber content and 25 mm length) has the lowest (μ) (5.53). One reason for the decrease in (μ) is the higher porous structure and lower density of banana fiber-reinforced geopolymers. The increase in voids in the material means that it will allow more vapor transmission. Allowing vapor transmission through a porous material is an important characteristic in terms of reducing

FIGURE 9. Digital images of the specimens (10x): reference specimen (a); 0.5–20 specimen (b); 0.5–25 specimen (c).

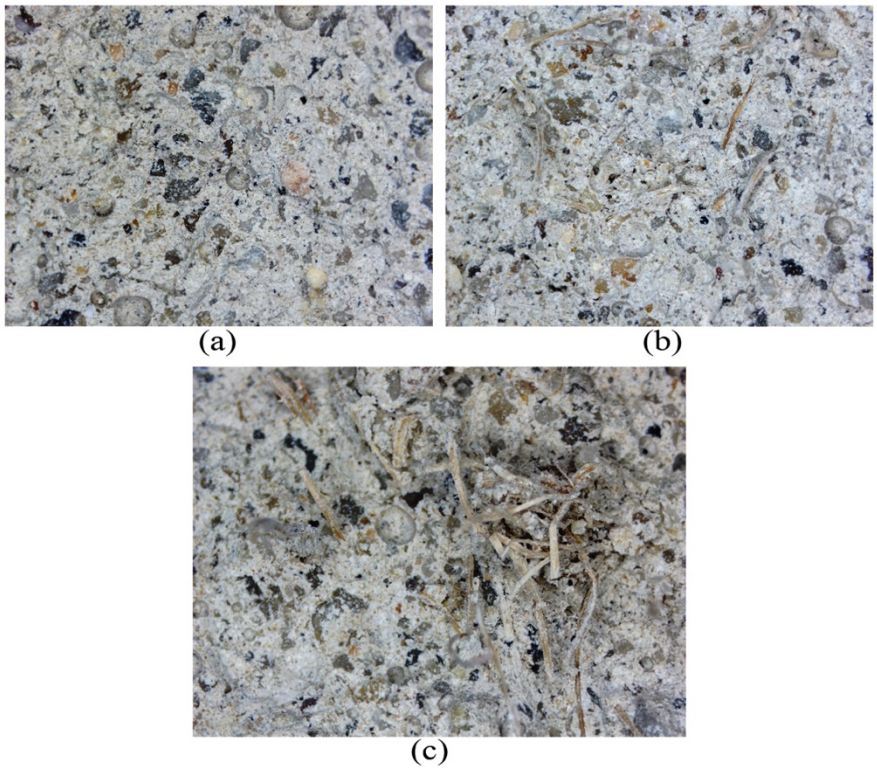

Downloaded from http://meridian.allenpress.com/jgb/article-pdf/19/1/51/3333621/i1943-4618-19-1-51.pdf by greenjournal@verizon.net on 02 March 2024

FIGURE 10. (WVDRI) of the mortars with 0.5, 1.0, and 1.5% fiber content as functions of fiber length.

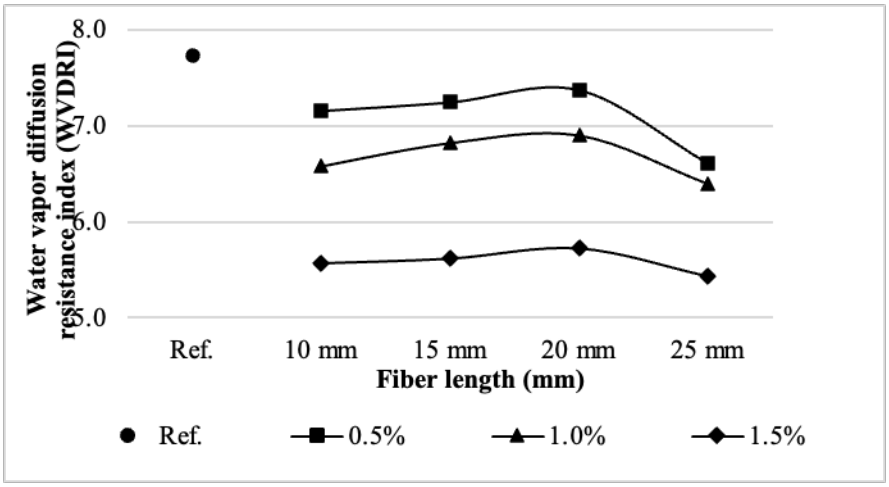

the risk of interstitial condensation. Otherwise, the condensed water would fill the voids in the material, deteriorating its structural stability and thermal insulation property.

The very slight upward trend in (μ) was negligible when the fiber length was increased from 10 mm to 20 mm, which may be accepted as the critical fiber length. However, further increasing the fiber length (to 25 mm) above the critical fiber length led to a sharp reduction in (μ). In all fiber contents (0.5, 1.0, and 1.5%), the lowest (μ) values were obtained at 25 mm fiber length. The main reason for this was that, as determined by other physical properties, the 25-mm banana fiber caused agglomeration which created more interstitial pores in the matrix. The (WVDRI) (μ) values of banana-fiber reinforced geopolymers compared with various conventional building materials are given in Table 3. As a result, the (μ) value of banana-fiber reinforced geopolymer mortars satisfies the requirement of the specification for nonload-bearing wall materials and mortars.

TABLE 3. The (WVDRI) (μ) values of banana-fiber reinforced geopolymers **compared with** various conventional building materials.

Material	WVDRI (μ)
Lime mortar [42]	<15
Lime-pozzolan mortar [42]	<15
Crushed brick-lime mortar [42]	<15
Hydraulic lime mortar [42]	<15
Cement mortar [43]	32
Fired clay brick [43, 44]	16–27
Aerated autoclaved concrete [43]	13
Banana-fiber reinforced geopolymers	**5.53–7.74**

Downloaded from http://meridian.allenpress.com/jgb/article-pdf/19/1/51/3333621/i1943-4618-19-1-51.pdf by greenjournal@verizon.net on 02 March 2024

3.1.6 Drying Shrinkage

Water has no part in the production of the geopolymer gel, in contrast to Portland cement [12]. The production of the geopolymer gel only requires a small quantity of water, known as "interstitial or structural water," but additional water, known as "free water," is added to the composition to make it workable. When this free water is lost, large deformations can result from shrinkage during drying [35]. The geopolymers have relatively large drying shrinkage which starts when the geopolymer reactions are finishing up [45] and results in tensile stress and interior cracks. The fibers in geopolymer mixtures can sustain this stress [12] and lower the concentration of stress at the crack tip, preventing the crack from growing further and preventing small cracks from combining to generate bigger ones [18]. The drying shrinkages of the entire population of the mortars as a function of the curing period of 90 days are presented in Figure 11.

According to Figure 11, the drying shrinkage was positively influenced by the introduction of banana fiber. Drying shrinkage values of the unreinforced reference mortar were reduced 0.46–0.88 times. In all fiber lengths (10, 15, 20, and 25 mm), when the fiber content increased from 0.5% to 1.5%, the drying shrinkage of the specimens were reduced. This behavior revealed the effectiveness of the increased fiber content in resisting the tensile stress occurring in the matrix, preventing crack formation and crack expansion. The decrease in shrinkage due to the increase in fiber content also coincided with the increase in the flexural and compressive strengths of the material as seen in Figure 12. As a matter of fact, it was stated in the literature that the mechanical properties of geopolymer composites reinforced with glass, polypropylene, and lignin-based fibers increased with decreasing shrinkage [18].

The shrinkage values decreased in the order of 25> 10> 15> 20 mm at the same fiber content. That is, when the fiber length increased from 10 to 15 and 20 mm, the gradual decrease in drying shrinkage indicated good resistance of the material under tensile stress until 20 mm fiber length. This result is in line with the other properties mentioned above. Again, in parallel to the results obtained for other properties, increasing the fiber length to 25 mm was insufficient to balance the mortar tensile stress because of the tendency of fibers to agglomerate and the

FIGURE 11. The drying shrinkages of the entire population of mortars as a function of the 90-day curing period.

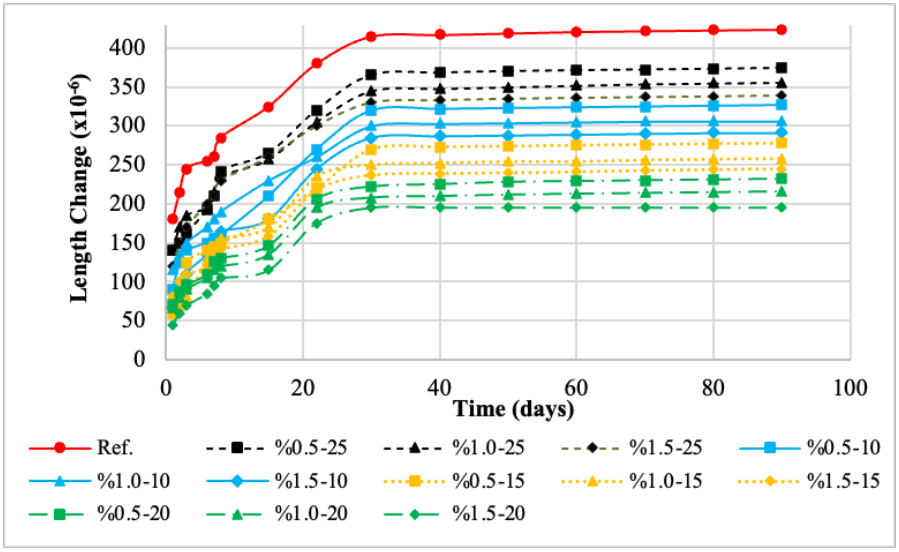

Downloaded from http://meridian.allenpress.com/jgb/article-pdf/19/1/51/3333621/i1943-4618-19-1-51.pdf by greenjournal@verizon.net on 02 March 2024

higher porosity of the matrix. In other words, the lower shrinkage of the fiber-reinforced material depends not only on the fiber content of the mortar but also on the optimum fiber length.

3.2 Effects of Fiber Content and Fiber Length on the Development of Mechanical Properties of Banana-Fiber Reinforced Geopolymers

3.2.1 Flexural Strength

The flexural and compressive strengths of the mortars with 0.5, 1.0, and 1.5% fiber content as functions of fiber length are given in Figure 12.

The lowest value of flexural strength (1.81 MPa) was found in the unreinforced reference geopolymer mortar that contained no banana fibers. Reinforcing the mortar with 0.5% banana fiber increased the flexural strength 2.36–3.21 times in the whole fiber lengths (10, 15, 20, and 25 mm) compared to the reference specimen. When the banana fiber content was increased to 1%, the increase in flexural strength was 2.52–3.52 times, and when the fiber content was increased to 1.5%, the increase in flexural strength was 2.66–3.80 times. In other words, more fiber incorporation positively affected the flexural strength of the mortar. The specimen with the highest banana fiber incorporation (1.5% fiber content) had the highest flexural strength of 6.88 MPa at each fiber length. The high tensile strength of the banana fiber, due to its effective interaction with the matrix, enabled the transmission of loads from the matrix to the fibers [17]. In addition, the increase in flexural strength demonstrated that the banana fibers could function as bridges between cracks and prevent further crack propagation. When a crack developed, the strength of the mortar declined and the matrix's bending stresses were transferred to the fibers. Because when a crack contacts with a fiber, a specific amount of energy is required to remove the fiber from the mortar, surpass adhesion, and lead to crack propagation through the entire matrix.

The "bridge effect" dispersed the stress among various sections of the specimen, preventing abrupt failure. When the material's capacity is once again exceeded by stresses in other regions,

FIGURE 12. Flexural and compressive strengths of the mortars with 0.5, 1.0, and 1.5% fiber content as functions of fiber length.

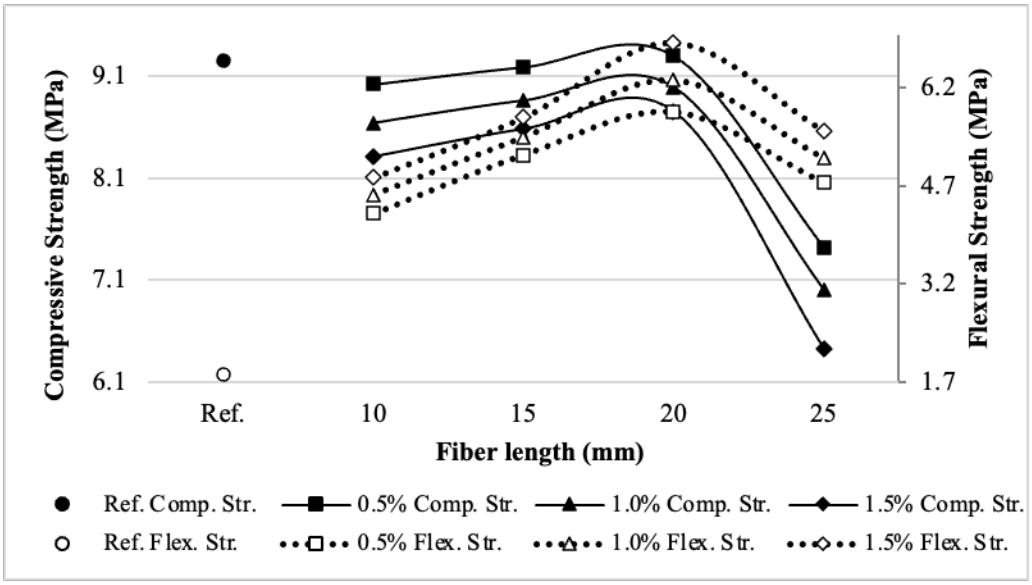

Downloaded from http://meridian.allenpress.com/jgb/article-pdf/19/1/51/3333621/i1943-4618-19-1-51.pdf by greenjournal@verizon.net on 02 March 2024

more cracks appear, and the process is repeated [35]. This finding is consistent with the findings of other studies in the literature. Wongsa et al. [17] determined that the incorporation of sisal and coconut fibers (up to 1.0 vol%) enhanced the flexural strength of fly ash-based geopolymer mortars. In another study, sisal and jute fibers (3 and 2 wt%, respectively) improved the flexural strength of an unreinforced geopolymer matrix approximately 4.3 and 4.1 times, respectively [16]. Furthermore, cotton (up to 0.5 wt%) [20, 21], lignin (up to 1.25 wt%) [18], and musa basjoo (up to 1.5 wt%) [19] fibers result in an increase in the flexural strength of fly ash/slag-based geopolymer binders.

When the effect of banana fiber length on flexural strength was evaluated, increasing the fiber length from 10 mm to 15 mm and 20 mm in the whole fiber contents (0.5, 1.0, and 1.5%) increased the flexural strength. The strength increasing until 20 mm fiber length may be ascribed to the fact that the extent of load transfer is a function of fiber length and the degree of interfacial adhesion between banana fiber and geopolymer matrix. Shorter fibers provide friction because of the higher number of fibers ends, while longer fibers provide higher deformation resistance [36]. The highest flexural strengths (5.82, 6.38, and 6.88 MPa, respectively) at fiber contents of 0.5, 1.0, and 1.5% were always obtained in specimens with fiber length of 20 mm. This finding was consistent with the findings obtained regarding physical properties. Therefore, the critical fiber length required for achieving stronger reinforcement in banana fiber-reinforced geopolymer mortars appears to be 20 mm. However, increasing the fiber length to 25 mm brought about a decrease in flexural strength. Agglomerations of fibers formed due to the presence of longer fibers in the matrix, weakening the interaction between matrix and fiber. However, the flexural strength of specimens with a fiber length of 25 mm was still higher than that of the reference specimen and specimens with a fiber length of 10 mm.

3.2.2 Compressive Strength

According to Figure 12, the highest compressive strength value (9.25 MPa) was found in the unreinforced geopolymer mortar that contained no banana fibers. In the whole fiber lengths (10, 15, 20, and 25 mm), reinforcing the mortar with 0.5% banana fiber reduced the (R_c) in the range of 9.02–7.42 MPa; with 1.0% banana fiber reduced the (R_c) in the range of 6.38–5.4.56 MPa; and with 1.5% banana fiber reduced the (R_c) in the range of 6.88–4.82 MPa. In other words, adding more fiber negatively affected the compressive strength of the mortar. The specimen with the highest banana fiber incorporation (1.5% fiber content) had the lowest compressive strength of 6.43 MPa.

Increasing the fiber length from 10 mm to 15 and 20 mm in the whole fiber contents (0.5, 1.0, and 1.5%) increased the compressive strength in parallel with the flexural strength. The highest compressive strengths at 0.5, 1.0, and 1.5% fiber contents (9.20, 8.99, and 8.75 MPa, respectively) were obtained in specimens with a fiber length of 20 mm. This finding was consistent with the findings obtained in terms of physical properties and revealed that at 20 mm fiber length the interaction between fibers and matrix reached its maximum degree. However, increasing the fiber length to 25 mm decreased the compressive strength, as determined by the flexural strength. The specimens with 25-mm banana fiber had the lowest compressive strengths of all fiber contents.

The fact that both the fiber ratio and the fiber length greater than the ideal value reduced the compressive strength due to: (i) the decreasing density of the material; (ii) a greater potential for fiber balling up, which decreased the fiber bridging mechanism [19]; and (iii) a higher void percentage inside the composite, which led to weaker zones inside the matrix [24]. However,

Downloaded from http://meridian.allenpress.com/jgb/article-pdf/19/1/51/3333621/i1943-4618-19-1-51.pdf by greenjournal@verizon.net on 02 March 2024

instead of increasing compressive strength, incorporating fibers are intended to improve ductility and stop cracks from propagating [35]. Therefore, as long as the material can maintain its integrity without deforming under load, the decrease in compressive strength can be negligible. This decreasing trend in compressive strength is also consistent with the results of other studies in the literature [23, 24, 46].

3.2.3 Toughness

Toughness is the area under the stress-strain curve and is an essential measure of the material's ability to absorb energy and withstand the propagation of cracks during plastic deformation under an applied load. The flexural load-displacement behavior of the mortars with 0.5, 1.0, and 1.5% fiber content as functions of fiber length is given in Figure 13.

Banana fiber had a substantial influence on how the mortars fractured. It is possible to see linear elastic deformation during the initial loading period. Microcracks developed as the load increased and the curve exhibited nonlinear deformation. Regardless of the fiber content and length, the peak loads of all fiber-reinforced specimens are higher than those of the unreinforced reference specimen, which also has the lowest area under the stress-strain curves. After peak load was reached, the descending curve for the unreinforced mortar dropped rapidly, exhibiting an abrupt and brittle failure form. In addition, the unreinforced matrix was completely broken under load, as shown in Figure 14a. As such, MoE of the reference mortar exhibited the highest value (9.55 GPa) due to this low deformation capacity.

On the other hand, more ductile behavior was detected in fiber-reinforced specimens. In contrast to the unreinforced matrix, fiber-reinforced specimens with a higher energy absorption

FIGURE 13. The influence of fiber lengths on the flexural load-displacement behavior of banana fiber-reinforced geopolymers: (a) at 0.5% fiber content; (b) at 1.0% fiber content; (c) at 1.5% fiber content.

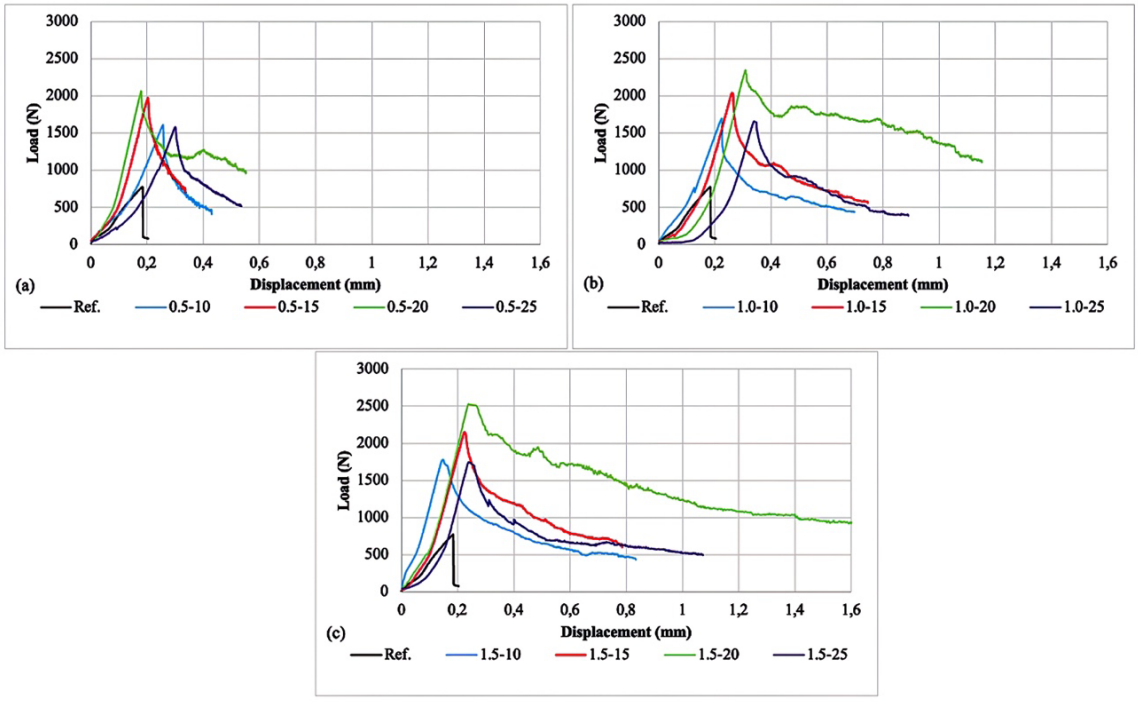

Downloaded from http://meridian.allenpress.com/jgb/article-pdf/19/1/51/3333621/i1943-4618-19-1-51.pdf by greenjournal@verizon.net on 02 March 2024

capacity (toughness) provided prolonged fractures with emerging signals that provided notice of the material's collapse [35]. The capacity of the geopolymer mortar to absorb energy increased with the increase in the amount of banana fiber present. Furthermore, increasing the fiber length from 10 mm to 20 mm increased the peak load and the area under the load vs displacement curve, indicating that the toughness improved gradually. However, increasing the fiber length to 25 mm caused a decrease in toughness, possibly because agglomerations of fibers inside the matrix weaken the interaction between matrix and banana fibers. Thus, the fibers were insufficient to avoid crack formation and propagation.

Geopolymer mortars reinforced with banana fibers maintained their shape after failure, as evidenced by the visual observations performed following the flexural strength tests and illustrated in Figure 14b. The pulled-out banana fiber imprints in this figure indicate strong adhesion between banana fibers and geopolymer matrix. The matrix was broken but the fibers protected it from disintegrating and kept the matrix together. In addition, the banana fibers had geopolymer products on their surfaces, which revealed a good adhesion (a strong interface) between the geopolymer matrix and the fibers (Figure 15).

4. CONCLUSION

The following conclusions could be drawn from the study findings when banana fibers are incorporated into geopolymer mortars:

- Plant-based banana fiber can be used in the production of geopolymers to improve their mechanical properties and ductility and to prevent the propagation of cracks.

FIGURE 14. The visual observations of the specimens after the flexural strength test: (a) unreinforced reference mortar (00–00 specimen); (b) banana fiber-reinforced geopolymer mortar (1.0–20 specimen).

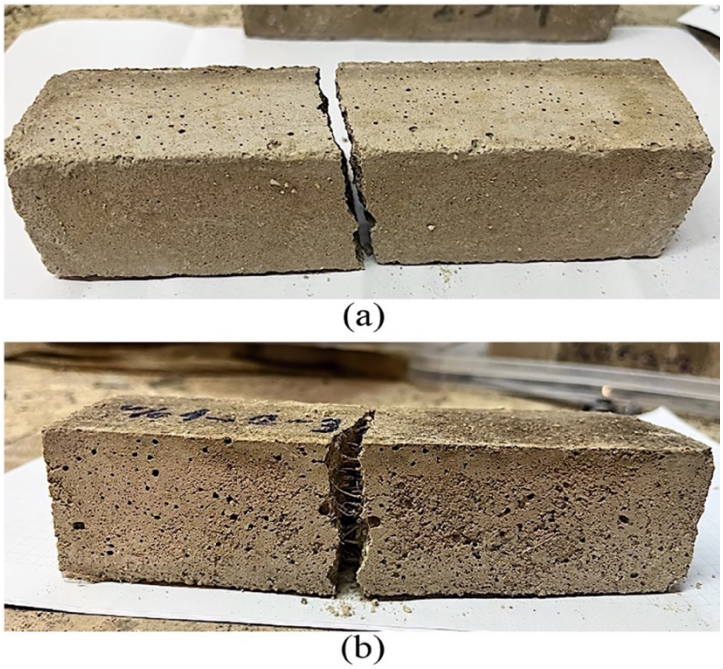

Downloaded from http://meridian.allenpress.com/jgb/article-pdf/19/1/51/3333621/i1943-4618-19-1-51.pdf by greenjournal@verizon.net on 02 March 2024

FIGURE 15. Geopolymer products detected on the surface of banana fibers.

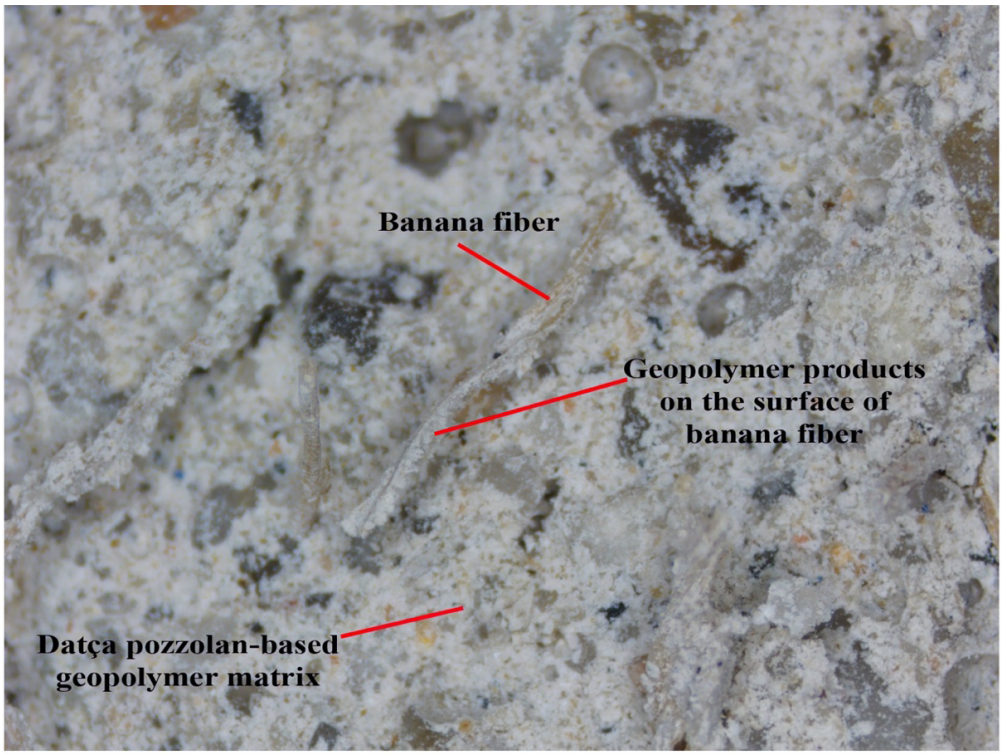

- By using this agricultural waste in geopolymer binders, the half-tonne of CO_2 emissions annually from each tonne of this waste can be saved.
- Fiber content and fiber length are critical parameters in the evolution of properties.
- Gradually increasing fiber content (up to 1.5% by weight) resulted in an increase in the porosity and water absorption ratios and a decrease in the workability, unit weight, ultrasound pulse velocity, modulus of elasticity and water vapor diffusion resistance index.
- The increase in fiber content improved the flexural strength, which reveals that the banana fiber effective interaction with the matrix enabled the transfer of loads and the ability of banana fibers to function as bridges between cracks and prevent further crack propagation.
- The increase in banana fiber length from 10 to 20 mm improved the properties of the specimens. This reveals that the interaction between banana fibers and geopolymer matrix reaches its maximum level at 20 mm fiber length which may be accepted as the critical fiber length. However, the increase in fiber length to 25 mm led to a sharp drop in all properties caused by lower dispersion and fiber agglomeration in the matrix.
- The stress-strain curve of the banana fiber-reinforced geopolymers did not abruptly decline when peak stress was achieved, and specimens displayed more ductile fracture behavior compared to unreinforced geopolymer mortar.
- The optimum banana fiber content and length were 1.5% and 20 mm, respectively, in terms of giving higher mechanical properties, ductility, and resistance to propagation of cracks.

Downloaded from http://meridian.allenpress.com/jgb/article-pdf/19/1/51/3333621/i1943-4618-19-1-51.pdf by greenjournal@verizon.net on 02 March 2024

ACKNOWLEDGEMENTS

The ITU Center for Scientific Research Projects [grant number FHD-2022-44014] provided funding for this work. The authors gratefully acknowledge the assistance of Ibrahim Oztürk and Gökhan Büyükkurt in Building Materials Laboratory, ITU, Faculty of Architecture.

REFERENCES

[1] N.B. Singh, B. Middendorf, Geopolymers as an alternative to Portland cement: An overview, Constr. Build. Mater. 237 (2020) 117455. https://doi.org/10.1016/j.conbuildmat.2019.117455.

[2] A. Garcia-Lodeiro, I. Palomo, A. Fernández-Jiménez, An overview of the chemistry of alkali-activated cement-based binders, in: F. Pacheco-Torgal, J.A. Labrincha, C. Leonelli, A. Palomo, P. Chindaprasirt (Eds.), Handbook of Alkali-Activated Cements, Mortars and Concretes, Woodhead Publishing, UK, 2015, pp. 19–47. Retrieved from https://doi.org/10.1533/9781782422884.1.19.

[3] K.Z. Farhan, M.A.M. Johari, R. Demirboğa, Assessment of important parameters involved in the synthesis of geopolymer composites: A review, Constr. Build. Mater. 264 (2020) 120276. https://doi.org/10.1016/j.conbuildmat.2020.120276.

[4] D. Bondar, C.J. Lynsdale, N.B. Milestone, N. Hassani, A.A. Ramezanianpour, Effect of type, form, and dosage of activators on strength of alkali-activated natural pozzolans, Cem. Concr. Compos. 33 (2011) 251–260. https://doi.org/10.1016/j.cemconcomp.2010.10.021.

[5] Z. Zhang, J.L. Provis, A. Reid, H. Wang, Geopolymer foam concrete: An emerging material for sustainable construction, Constr. Build. Mater. 56 (2014) 113–127. https://doi.org/10.1016/j.conbuildmat.2014.01.081.

[6] RILEM TC 224-AAM, State-of-the-art report, Alkali Activated Materials, 2014, Retrieved January 27, 2018, from DOI 10.1007/978-94-007-7672-2_6.

[7] G. Habert, J.B. d'Espinose de Lacaillerie, N. Roussel, An environmental evaluation of geopolymer based concrete production: reviewing current research trends, J. Clean. Prod. 19(11) (2011) 1229–1238. https://doi.org/10.1016/j.jclepro.2011.03.012.

[8] J. Davidovits, Geopolymer Chemistry and Applications, fifth ed., Institut Géopolymère, Saint-Quentin, 2011.

[9] J.L. Provis, S.A. Bernal, Geopolymers and related alkali-activated materials, Annu. Rev. Mater. Res. 44 (2014) 299–327. http://dx.doi.org/10.1146/annurev-matsci-070813-113515.

[10] G. Zheng, X. Cui, W. Zhang, Z. Tong, Preparation of geopolymer precursors by sol–gel method and their characterization, J. Mater. Sci. 44 (2009) 3991–3996. http://dx.doi.org/10.1007/s10853-009-3549-x.

[11] M.I. Abdul Aleem, P.D. Arumairaj, Geopolymer concrete—A review, Int. J. Eng. Sci. Emerg. Technol. 1(2) (2012) 118–122. http://dx.doi.org/10.7323/ijeset/v1_i2_14.

[12] A.G.N. Abbas, F.N.A. Abdul Aziz, K. Abdan, N.A.M. Nasir, G.F. Huseien, A state-of-the-art review on fibre-reinforced geopolymer composites, Constr. Build. Mater. 330 (2022) 127187. https://doi.org/10.1016/j.conbuildmat.2022.127187.

[13] G. Silva, S. Kim, R. Aguilar, J. Nakamatsu, Natural fibers as reinforcement additives for geopolymers—a review of potential eco-friendly applications to the construction industry, Sustain. Mater. Technol. 23 (2020) e00132. https://doi.org/10.1016/j.susmat.2019.e00132.

[14] M.I.M. Alzeer, K.J.D. MacKenzie, Fiber composites of inorganic polymers (geopolymers) reinforced with natural fibers, in: I.M. Low, Y. Dong (Eds.), Compos. Mater. Elsevier, 2021, pp. 117–147. https://doi.org/10.1016/B978-0-12-820512-9.00016-2.

[15] H.Y. Ersoy, Kompozit Malzeme, fourth ed., Literatür Yayınları, Istanbul, 2001.

[16] G. Silva, S. Kim, B. Bertolotti, J. Nakamatsu, R. Aguilar, Optimization of a reinforced geopolymer composite using natural fibers and construction wastes, Constr. Build. Mater. 258 (2020) 119697. https://doi.org/10.1016/j.conbuildmat.2020.119697.

[17] A. Wongsa, R. Kunthawatwong, S. Naenudon, V. Sata, P. Chindaprasirt, Natural fiber reinforced high calcium fly ash geopolymer mortar, Constr. Build. Mater. 241 (2020) 118143. https://doi.org/10.1016/j.conbuildmat.2020.118143.

[18] Z. Su, L. Guo, Z. Zhang, P. Duan, Influence of different fibers on properties of thermal insulation composites based on geopolymer blended with glazed hollow bead, Constr. Build. Mater. 203 (2019) 525–540. https://doi.org/10.1016/j.conbuildmat.2019.01.121.

Downloaded from http://meridian.allenpress.com/jgb/article-pdf/19/1/51/3333621/i1943-4618-19-1-51.pdf by greenjournal@verizon.net on 02 March 2024

[19] Y.B.S. Reddy, S. Praburanganathan, M. Mishra, Experimental investigation on the fiber reinforced ash-based geopolymer concrete with musa basjoo fibers, Mater. Today: Proc. 65(8) (2022) 3700–3706. https://doi.org/10.1016/j.matpr.2022.06.297.
[20] T. Alomayri, I.M. Low, Synthesis and characterization of mechanical properties in cotton fiber-reinforced geopolymer composites, J. Asian Ceram. Soc. 1(1) (2013a) 30–34. https://doi.org/10.1016/j.jascer.2013.01.002.
[21] T. Alomayri, F.U.A. Shaikh, I.M. Low, Characterisation of cotton fibre-reinforced geopolymer composites, Compos. B. Eng. 50 (2013b) 1–6. https://doi.org/10.1016/j.compositesb.2013.01.013.
[22] B. Poletanovic, J. Dragas, I. Ignjatovic, M. Komljenovic, I. Merta, Physical and mechanical properties of hemp fibre reinforced alkali-activated fly ash and fly ash/slag mortars, Constr. Build. Mater. 259 (2020) 119677. https://doi.org/10.1016/j.conbuildmat.2020.119677.
[23] R.Y. Nkwaju, J.N.Y. Djobo, J.N.F. Nouping, P.W.M. Huisken, J.G.N. Deutou, L. Courard, Iron-rich laterite-bagasse fibers based geopolymer composite: mechanical, durability and insulating properties, Appl. Clay Sci. 183 (2019) 105333. https://doi.org/10.1016/j.clay.2019.105333.
[24] R.N. Yanou, R.C. Kaze, A. Adesina, J.G.D. Nemaleu, S.B.K. Jiofack, J.N.Y. Djobo, Performance of laterite-based geopolymers reinforced with sugarcane bagasse fibers, Case Stud. Constr. Mater. 15 (2021) e00762. https://doi.org/10.1016/j.cscm.2021.e00762.
[25] M. Mostafa, N. Uddin, Effect of banana fibers on the compressive and flexural strength of compressed earth blocks, Building. 5 (2015) 282–296. http://dx.doi.org/10.3390/buildings5010282.
[26] H.A. Santana, N.S.A. Júnior, D.V. Ribeiro, M.S. Cilla, C.M.R. Dias, Vegetable fibers behavior in geopolymers and alkali-activated cement based matrices: A review, J. Build. Eng. 44 (2021) 103291. https://doi.org/10.1016/j.jobe.2021.103291.
[27] TS EN 12350-5, Testing fresh concrete—Part 5: Flow table test, Turkish Standard Institution, Ankara, 2019.
[28] TS EN 1015-10, Methods of test for mortar for masonry—Part 10: Determination of dry bulk density of hardened mortar, Turkish Standard Institution, Ankara, 2001.
[29] TS EN 13755, Natural stone test methods—Determination of water absorption at atmospheric pressure, Turkish Standard Institution, Ankara, 2009.
[30] ISO 8335, Cement-bonded particleboards—boards of portland or equivalent cement reinforced with fibrous woodparticles, International Organization for Standardization, 1987.
[31] TS EN 14579, Natural stone test methods—Determination of sound speed propagation, Turkish Standard Institution, Ankara, 2006.
[32] TS EN 1920-8, Testing of concrete—Part 8: Determination of drying shrinkage of concrete for samples prepared in the field or in the laboratory, Turkish Standard Institution, Ankara, 2009.
[33] TS EN 12086, Thermal insulating products for building applications-Determination of long term water absorption by immersion, Turkish Standard Institution, Ankara, 2013.
[34] TS EN 196-1, Methods of testing cement—Part 1: Determination of strength, Turkish Standard Institution, Ankara, 2009.
[35] A.R.G. Azevedo, A.S.A. Cruz, M.T. Marvila, L.B. de Oliveira, S.N. Monteiro, C.M.F. Vieira, R. Fediuk, R. Timokhin, N. Vatin, M. Daironas, Natural fibers as an alternative to synthetic fibers in reinforcement of geopolymer matrices: A comparative review, Polymer. 13 (2021) 2493. https://doi.org/10.3390/polym13152493.
[36] T. Lin, D. Jia, P. He, M. Wang, D. Liang, Effects of fiber length on mechanical properties and fracture behavior of short carbon fiber reinforced geopolymer matrix composites, Mater. Sci. Eng. A. 497(1–2) (2008) 181–185. https://doi.org/10.1016/j.msea.2008.06.040.
[37] T. Alomayri, H. Assaedi, F.U.A. Shaikh, I.M. Low, Effect of water absorption on the mechanical properties of cotton fabric-reinforced geopolymer composites, J. Asian Ceram. Soc. 2(3) (2014) 223–230. https://doi.org/10.1016/j.jascer.2014.05.005.
[38] M.M. Camargo, E. Adefrs Taye, J.A. Roether, D. Tilahun Redda, A.R. Boccaccini, A review on natural fiber-reinforced geopolymer and cement-based composites, Material. 13 (2020) 4603. https://doi.org/10.3390/ma13204603.
[39] H.N. Dhakal, Z.Y. Zhang, M.O.W. Richardson, Effect of water absorption on the mechanical properties of hemp fibre reinforced unsaturated polyester composites, Compos. Sci. Technol. 67 (2007) 1674–1683. https://doi.org/10.1016/j.compscitech.2006.06.019.
[40] M.K. Lim, H. Cao, Combining multiple NDT methods to improve testing effectiveness, Constr. Build. Mater. 38 (2013) 1310–1315. https://doi.org/10.1016/j.conbuildmat.2011.01.011.

Downloaded from http://meridian.allenpress.com/jgb/article-pdf/19/1/51/3333621/i1943-4618-19-1-51.pdf by greenjournal@verizon.net on 02 March 2024

[41] A. Hajimohammadi, T. Ngo, P. Mendis, A. Kashani, J.S.J. van Deventer, Alkali activated slag foams: The effect of the alkali reaction on foam characteristics, J. Clean. Prod. 147 (2017) 330–339. https://doi.org/10.1016/j.jclepro.2017.01.134.
[42] E. Sassoni, P. Pahlavan, E. Franzoni, M.C. Bignozzi, Valorization of brick waste by alkali-activation: A study on the possible use for masonry repointing, Ceram. Int. 42(13) (2016) 14685–14694. https://doi.org/10.1016/j.ceramint.2016.06.093.
[43] E. Gürdal, D. Malïk, G. Akinci, Yapı malzemelerinin buhar geçirgenliği direnç katsayısının ölçülmesi, Restorasyon ve Konservasyon Çalışmaları Dergisi. 10 (2013) 48–52.
[44] L. Tanaçan, Hafif duvar tuğlası üretiminde perlit ve bazı katkıların etkilerinin araştırılması, Doktora Tezi, Istanbul Teknik Üniversitesi Fen Bilimleri Enstitüsü, Istanbul, 1993.
[45] K.Z. Farhan, M.A.M. Johari, R. Demirboğa, Impact of fiber reinforcements on properties of geopolymer composites: A review, J. Build. Eng. 44 (2021) 102628. https://doi.org/10.1016/j.jobe.2021.102628.
[46] R. Chen, S. Ahmari, L. Zhang, Utilization of sweet sorghum fiber to reinforce fly ash-based geopolymer, J. Mater. Sci. 49 (2014) 2548–2558. https://doi.org/10.1007/s10853-013-7950-0.
[47] BS EN 1062-1, Paints and varnishes. Coating materials and coating systems for exterior masonry and concrete, Classification, 2004.
[48] TS 699, Natural building stones—Methods of inspection and laboratory testing, Turkish Standard Institution, Ankara, 2009.

Downloaded from http://meridian.allenpress.com/jgb/article-pdf/19/1/51/3333621/i1943-4618-19-1-51.pdf by greenjournal@verizon.net on 02 March 2024

Downloaded from http://meridian.allenpress.com/jgb/article-pdf/19/1/51/3333621/i1943-4618-19-1-51.pdf by greenjournal@verizon.net on 02 March 2024

About the Editors

Co-Editors-in-Chief

Simi Hoque, Ph.D.
Civil, Architectural, and Environmental Engineering
Drexel University
https://simi734.wixsite.com/simi



Jian Zuo, Ph.D.
School of Architecture and Built Environment
The University of Adelaide
https://www.adelaide.edu.au/directory/Jian.Zuo



Recognised as a leading national researcher in Sustainable Development in the Australian's Research Awards 2023.

Advisory Board

Cathryn Copper

Head, Eberhard Zeidler
Architecture Library
University of Toronto



Mark Gorgolewski, Ph.D.
Department of Architectural Science
Ryerson University



Giuliana Iannaccone, Ph.D.
Department of Architecture & Construction
Politecnico di Milano



David Sailor, Ph.D.
Director, Urban Climate Research Center
Arizona State University



Professor Geoffrey Q.P. Shen
Chair Professor of Construction Management
The Hong Kong Polytechnic University



Professor Jianzhuang Xiao
College of Civil Engineering
Tongji University



Editorial Assistant

Mr. Daniel Oteng
University of Adelaide, Australia

Senior Editorial Board

Lola Ben-Alon, Ph.D.
Graduate School of Architecture, Planning and Preservation
Columbia University

Edwin H W Chan, Ph.D.
Building and Real Estate Department
The Hong Kong Polytechnic University

Qian (Victoria) Chen, Ph.D.
Construction Systems Management
The Ohio State University

Tom Collins, Ph.D.
Department of Architecture
Ball State University

Corey Griffin, Ph.D.
Associate Dean & Professor of Architecture
Penn State Altoona

Matthias Haase, Ph.D.
Institute for Facility Management
Zurich University of Applied Sciences

Liv M. Haselbach, Ph.D.
Department of Civil and Environmental Engineering
Lamar University

Erin Hopkins, Ph.D.
Department of Property Management
Virginia Polytechnic University

Ming Hu, Assistant Professor
School of Architecture, Planning & Preserveration
University of Maryland

Lotte Bjerregaard Jensen, Ph.D.

Department of Civil Engineering
Technical University of Denmark

Karen Kensek, Professor of Practice
School of Architecture
University of Southern California

Oliver Kinnane, Ph.D.
Architecture Planning & Environmental Policy
University College Dublin

Sandeep Langar, Ph.D.
Department of Construction Science
University of Texas at San Antonio

Wilson W.S. Lu, Ph.D.
Department of Real Estate and Construction
The University of Hong Kong

Colin MacDougall, Ph.D.
Department of Civil Engineering
Queen's University

Mikesch Muecke, Ph.D.
Architecture Department
Iowa State University

Masa Noguchi, Ph.D.
Faculty of Architecture, Building & Planning
The University of Melbourne

Christine O'Hara, Associate Professor
Landscape Architecture Department
California Polytechnic State University

Annie Pearce, Ph.D.
Myers-Lawson School of Construction
Virginia Tech

Emina Petrovic, Ph.D.

School of Architecture
Victoria University of Wellington

Tiziano Li Piani, Ph.D.
Civil Engineering
Technical University of Delft (TUD)

Svetlana Pushkar, Ph.D.
Department of Civil Engineering
Ariel University

Raviduth Ramful, Ph.D.
Faculty of Engineering
University of Mauritius

Alan Richardson, Ph.D.
School of the Built Environment
Northumbria University

Brian A. Rock, Ph.D.
Department of Civil, Environmental and
Architectural Engineering
The University of Kansas

Monica Rossi-Schwarzenbeck, Ph.D.
College of Civil Engineering
Leipzig University of Applied Sciences

Friedrich Sick, Ph.D.
FHTW Berlin
University of Applied Sciences

Brett Tempest, Ph.D.
Department of Civil and Environmental
Engineering
University of North Carolina at Charlotte

Zezhou Wu, Ph.D.
College of Civil and Transportation Engineering
Shenzhen University

Eunhwa Yang, Ph.D.
School of Building and Construction
Georgia Institute of Technology

Editorial Board Members

Dr. Ruidong Chang
The University of Adelaide, Australia

Dr. Hanliang Fu
Xi'an University of Architecture and Technology,
China

Dr. Yilong Han
Tongji University, China

Dr. Jian Li Hao
Xi'an Jiaotong-Liverpool University, China

Dr. Wengui Li
University of Technology Sydney, Australia

Dr. Chao Mao
Deputy Head, School of Management Science and
Real Estate
Chongqing University

Dr. Kim Maund
Deputy Head of School, School of Architecture
and Built Environment
The University of Newcastle

Dr. Neda Sadeghi
Department of Construction Science
Texas A&M University

Dr. Nilupa Udawatta
Deakin University, Australia

Dr. Ge Wang
Huanzhong Agricultural University, China

Professor Tao Wang
Chongqing University, China

Dr. Dujuan Yang
Department of the Built Environment
Eindhoven University of Technology

Dr. Xueliang Yuan
Shandong University, China

Professor Jingxiao Zhang
Chang'An University, China

Dr. Xianbo Zhao
Central Queensland University, Australia

JOURNAL OF greenbuilding
College Publishing

eISSN: 1943-4618 **ISSN:** 1552-6100

General Inform...
Web of Science ...
Journal Citatio...
Peer Review Inf...
PubMed® Infor...

Return to Search Results

JOURNAL OF GREEN BUILDING

Share This Journal

ISSN / eISSN **1552-6100 / 1943-4618**
Publisher **COLLEGE PUBLISHING, 12309 LYNWOOD DR, GLEN ALLEN, USA, VA, 23059**

General Information

Journal Website	Visit Site	**Publisher Website**	Visit Site
1st Year Published	2006	**Frequency**	Quarterly
Issues Per Year	4	**Country / Region**	UNITED STATES OF AMERICA
Primary Language	English		

Web of Science Coverage

Collection	Index	Category	Similar Journals
Core Collection	Arts & Humanities Citation Index (AHCI)	Architecture	Find Similar Journals
Current Contents	Arts & Humanities	Art & Architecture	Find Similar Journals

Search a topic within this journal

Search a topic within this journal...

Search

Journal Citation Report™ (JCR)

Journal Citation Repor

Journal Impact Factor™ (JIF)

JCR SUBSCRIPTION ACTIVE

2023	2022

Downloaded on 10.03.2025 11:09:55

2023 Journal Performance Data for: Journal of Green Building

ISSN
1552-6100

EISSN
1943-4618

JCR ABBREVIATION
J GREEN BUILD

ISO ABBREVIATION
J. Green Build.

Journal Information

EDITION
Arts & Humanities Citation Index (AHCI)

CATEGORY
ARCHITECTURE

LANGUAGES
English

REGION
USA

1ST ELECTRONIC JCR YEAR
2020

Publisher Information

PUBLISHER
COLLEGE PUBLISHING

ADDRESS
12309 LYNWOOD DR, GLEN ALLEN, VA 23059

PUBLICATION FREQUENCY
4 issues/year

 © 2025 Clarivate

Rank by Journal Impact factor

Note: While journals indexed in AHCI and ESCI receive a JIF from the 2022 release in June 2023 onward, journals in the 25 arts & humanities categories will not receive ranks, quartiles, or percentiles.Learn more

Rank by Journal Citation Indicator (JCI)

Journals within a category are sorted in descending order by Journal Citation Indicator (JCI) resulting in the Category Ranking below. A separate rank is shown for each category in which the journal is listed in JCR. Data for the most recent year is presented at the top of the list, with other years shown in reverse chronological order.Learn more

CATEGORY

ARCHITECTURE

8/97

JCR YEAR	JCI RANK	QUARTILE	JCI PERCENTILE
2023	8/97	Q1	92.27
2022	4/97	Q1	96.39
2021	5/93	Q1	95.16
2020	7/91	Q1	92.86
2019	7/90	Q1	92.78
2018	8/88	Q1	91.48
2017	11/87	Q1	87.93

 © 2025 Clarivate

JOURNAL OF
greenbuilding

VOLUME 19 NUMBER 1 **WINTER 2024**

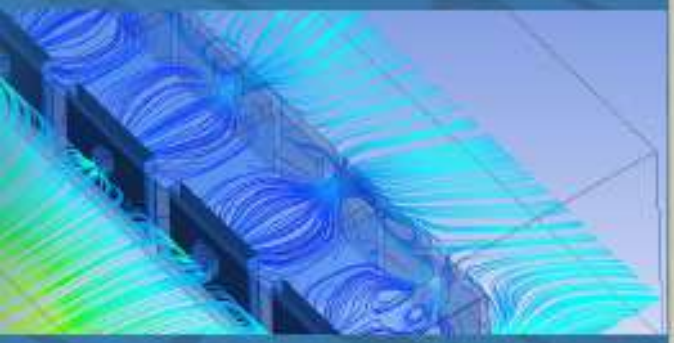





IN THIS ISSUE

RESEARCH ARTICLES

Effect and Mechanism of China's Prefabricated Building Policies to Promote Patent Output with Carbon-Neutrality as a Target *Layin Wang, Jinrong Zhang, Xin Lei, and Bozheng Yang*

Using Deep Learning to Optimize HVAC Systems in Residential Buildings *Tran Van Quang, Nguyen Lu Phuong*

Performance of Natural Pozzolan-Based Geopolymer Reinforced with Banana Fibers *Kübra Ekiz Bariş, Leyla Tanaçan*

Asymmetric Flexural Behavior of Glulam Beams Based on Bamboo-Inspired Functionally Graded Structure for High Bending Load Applications *Raviduth Ramful*

Sustainable Retrofitting Strategies for Culturally Significant Brutalist Buildings: Energy-Efficient Strategies for a High-Rise Residential Complex in Sarajevo, Bosnia and Herzegovina *Suncica Milosevic, Ajla Aksamija Ph.D.*

A Case Study: Intelligent Shading Retrofit to Existing Home-Office using Multi-Objective Optimization *Tajik, Ramyar, Soltanmohammadlou, Saeideh, Kianfar, Amir, Masera, Gabriele, Hoque, Simi*

Optimization of Visual Comfort in Office Space Based on Stochastic Shade Adjustment *Zhang Yijie and Yao Jian*

Indoor Environmental Quality In Preschool Buildings In an Andean City In Ecuador *Angélica Ochoa-Avilés, Andrea Parra-Ullauri, María José Jaramillo-Torres, Samuel Escandón, Mayra Parra-Ullauri, Danilo Mejía, Cristina Ochoa-Avilés, Claudia Rodas-Espinoza*

A Study on the Evaluation Methods of Indoor Light Environment for Occupant Comfort and Well-being *Ki Rim Kim, Kyung Sun Lee, and Jaewook Lee*

An Agent-Based Computational Model on Household Electricity Consumption in Indian Cities *Manas Vijayan, Akshay Patil, Vijay Kapse*

Dormitory Environment, Learning Engagement, and College Students' Mental Health: An Empirical Study of Survey Data from 45 Universities in China *Wenya Huang, Wanting Liu, Min Zeng, and Zhenhua Zheng*

Investigating LEED-ND Key Criteria for Effective Sustainability Evaluation *Mohsen Goodarzi and George Berghorn*

How Different Types of Knowledge Affect the Energy-Saving Intention of College Students—Evidence from Eye-Tracking Experiments *Menglin Xing, Xi Luo, Xiaojun Liu, and Na Li*

Issues

Select Year 2024

Select Issue Winter - Volume 19, Issue 1

RESEARCH ARTICLES

EFFECT AND MECHANISM OF CHINA'S PREFABRICATED BUILDING POLICIES TO PROMOTE PATENT OUTPUT WITH CARBON-NEUTRALITY AS A TARGET

Layin Wang; Jinrong Zhang; Xin Lei; Bozheng Yang

Abstract View Article PDF

USING DEEP LEARNING TO OPTIMIZE HVAC SYSTEMS IN RESIDENTIAL BUILDINGS

Tran Van Quang; Nguyen Lu Phuong

Abstract View Article PDF

PERFORMANCE OF NATURAL POZZOLAN-BASED GEOPOLYMER REINFORCED WITH BANANA FIBERS

Kübra Ekiz Bariş; Leyla Tanaçan

Abstract View Article PDF

Get Email Alerts

Latest Issue Alert

Latest Most Read Most Cited

EFFECT AND MECHANISM OF CHINA'S PREFABRICATED BUILDING POLICIES TO PROMOTE PATENT OUTPUT WITH CARBON-NEUTRALITY AS A TARGET
Layin Wang, Jinrong Zhang, Xin Lei, Bozheng Yang

USING DEEP LEARNING TO OPTIMIZE HVAC SYSTEMS IN RESIDENTIAL BUILDINGS
Tran Van Quang, Nguyen Lu Phuong

DORMITORY ENVIRONMENT, LEARNING ENGAGEMENT, AND COLLEGE STUDENTS' MENTAL HEALTH: AN EMPIRICAL STUDY OF SURVEY DATA FROM 45 UNIVERSITIES IN CHINA
Wenya Huang, Wanting Liu, Min Zeng, Zhenhua Zheng

A STUDY ON THE EVALUATION METHODS OF INDOOR LIGHT ENVIRONMENT FOR OCCUPANT COMFORT AND WELL-BEING
Ki Rim Kim, Kyung Sun Lee, Jaewook Lee

Indoor Environmental Quality In Preschool Buildings In an Andean City

ASYMMETRIC FLEXURAL BEHAVIOR OF GLULAM BEAMS BASED ON BAMBOO-INSPIRED FUNCTIONALLY GRADED STRUCTURE FOR HIGH BENDING LOAD APPLICATIONS

Raviduth Ramful

Abstract | View Article | PDF

SUSTAINABLE RETROFITTING STRATEGIES FOR CULTURALLY SIGNIFICANT BRUTALIST BUILDINGS: ENERGY-EFFICIENT STRATEGIES FOR A HIGH-RISE RESIDENTIAL COMPLEX IN SARAJEVO, BOSNIA AND HERZEGOVINA

Suncica Milosevic; Ajla Aksamija, Ph.D.

Abstract | View Article | PDF

A CASE STUDY: INTELLIGENT SHADING RETROFIT TO EXISTING HOME-OFFICE USING MULTI-OBJECTIVE OPTIMIZATION

Ramyar Tajik; Saeideh Soltanmohammadlou; Amir Kianfar; Gabriele Masera; Simi Hoque

Abstract | View Article | PDF

OPTIMIZATION OF VISUAL COMFORT IN OFFICE SPACE BASED ON STOCHASTIC SHADE ADJUSTMENT

Zhang Yijie; Yao Jian

Abstract | View Article | PDF

In Ecuador

Angélica Ochoa-Avilés, Andrea Parra-Ullauri, María José Jaramillo-Torres, Samuel Escandón, Mayra Parra-Ullauri, Danilo Mejía, Cristina Ochoa-Avilés, Claudia Rodas-Espinoza

Volume 19, Issue 1

Winter 2024



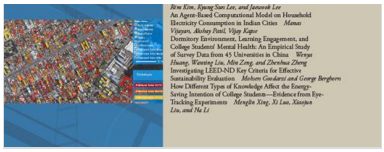

ISSN 1552-6100

eISSN 1943-4618

In this Issue

RESEARCH ARTICLES

Indoor Environmental Quality In Preschool Buildings In an Andean City In Ecuador

Angélica Ochoa-Avilés; Andrea Parra-Ullauri; María José Jaramillo-Torres; Samuel Escandón; Mayra Parra-Ullauri; Danilo Mejía; Cristina Ochoa-Avilés; Claudia Rodas-Espinoza

Abstract | View Article

PDF

A STUDY ON THE EVALUATION METHODS OF INDOOR LIGHT ENVIRONMENT FOR OCCUPANT COMFORT AND WELL-BEING

Ki Rim Kim; Kyung Sun Lee; Jaewook Lee

Abstract | View Article

PDF

AN AGENT-BASED COMPUTATIONAL MODEL ON HOUSEHOLD ELECTRICITY CONSUMPTION IN INDIAN CITIES

Manas Vijayan; Akshay Patil; Vijay Kapse

Abstract | View Article

PDF

DORMITORY ENVIRONMENT, LEARNING ENGAGEMENT, AND COLLEGE STUDENTS' MENTAL HEALTH: AN EMPIRICAL STUDY OF SURVEY DATA FROM 45 UNIVERSITIES IN CHINA

Wenya Huang; Wanting Liu; Min Zeng; Zhenhua Zheng

Abstract | View Article

PDF

INVESTIGATING LEED-ND KEY CRITERIA FOR EFFECTIVE SUSTAINABILITY EVALUATION

Mohsen Goodarzi; George Berghorn

Abstract View Article

PDF

HOW DIFFERENT TYPES OF KNOWLEDGE AFFECT THE ENERGY-SAVING INTENTION OF COLLEGE STUDENTS—EVIDENCE FROM EYE-TRACKING EXPERIMENTS

Menglin Xing; Xi Luo; Xiaojun Liu; Na Li

Abstract View Article

PDF

Cover Image

All Issues

JOURNAL OF greenbuilding

College Publishing

eISSN: 1943-4618 **ISSN:** 1552-6100

Privacy Policy Get Adobe Acrobat Reader Support